UNIVERSITÀ DI TRENTO
CIBIO
Dipartimento di
Biologia Cellulare, Computazionale e Integrata

PhD program 33rd cycle

Microbial enzymes for hair removal: an integrated biotechnological approach for application in the leather tanning industry

Supervisor:

Alessandro Quattrone

PhD student:

Elisa Demattè

Advisor:

Olivier Jousson

Accademic year 2019/2020

Dedicated to my grandpa, Fabio,

who left me too early.

Love you.

ABBREVIATIONS

BOD: Biochemical Oxygen Demand

CFU: Colonies forming unit

COD: Chemical Oxygen Demand

DNTB: 5,5'-dithiobis-(2-nitrobenzoic acid)

FMM: Feather Minimal Medium

KA: Keratin Azure

NA: Nutrient Agar

NB: Nutrient Broth

NGS: Next Generation Sequencing

OD: Optical Density

TCA: Trichloroacetic acid

TDS: Total Dissolved Solid

WMM: Wool Minimal Medium

ABSTRACT

Microbial enzymes have been used for decades in a number of processes in the industrial, biomedical, environmental, and agro-food sectors. The dehairing phase of the leather tanning process is currently mediated by sulphur/sulphides chemicals, requiring expensive and complex procedures for water depollution and increasing safety risks for workers. This project is aimed at the development of a microbially-driven process for hair removal based on secreted enzymes. The first phase of the project consisted in the isolation of microorganisms naturally present on raw hides (cow skin) and displaying dehairing ability. A collection of 52 pure bacterial isolates was first screened for proteolytic activity (25 positive isolates) and then for their ability to grow on minimal media (10 positive isolates). The genome of these 10 isolates was sequenced and the supernatants containing secreted enzymes (and potential other metabolites) were tested for enzymatic activity and dehairing capacity at a laboratory scale. The secretome analysis reported the presence of more than 200 secreted proteins for each isolate and showed an increase in the release of hydrolytic enzymes during growth on minimal media. Further selection among the 10 isolates was based on proteomic analysis, pilot scale dehairing tests and yields after the downstream process

The 4 isolates, selected on the base of the unhairing ability, secretome analysis and downstream yields, were subjected to further characterization to choose the most promising for the desired activity. Isolate 1Dm15, selected for the dehairing ability demonstrated at pilot scale, was grown in bioreactor and once the parameters were defined a scale-up of the process was performed.

In conclusion, in this work we identified a *Bacillus sp*. strain able to grow on minimal media and secrete a pool of enzymes active in the dehairing of hides. This microbially driven process shows promising application in the industrial practice substituting the use of reducing agents.

INTRODUCTION

SKIN COMPOSITION

Animal skin is a complex structure, which protects the environment and temperature control, but it is also an extended organ able to contain the mass of big animals (Figure 1).

At molecular level, the composition of skin is complex and present many details. The most important protein is collagen, which represents a large family of 28 proteins. All of them have specific characteristics and are present at different concentrations in all layers that constitute the skin.

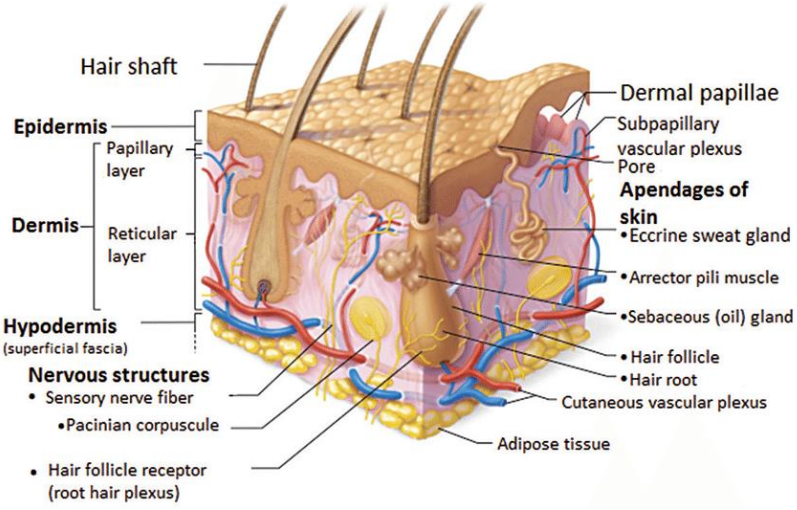

Figure 1- structure and layers of skin (Marieb, *et al.*, 2006)

EPIDERMIS

The outermost layer in the skin is the epidermis, composed mainly of keratin. It is divided into four layers: stratum corneum at the top composed of non-viable keratinocytes and corneocytes, stratum granulosum containing non-dividing keratinocytes, stratum spinosum with low dividing keratinocytes and the stratum basale directly connected to the basement membrane and containing high dividing keratinocytes and melanocytes.

The most abundant protein is keratin, which is present in all layers at different concentrations: 80% stratum corneum and 30% stratum basale (Cantera, 2001). Keratin (Figure 2) is a fibrous and structural protein strongly stabilized by disulfide linkages. Based on the secondary structure, it is named alpha

keratin, based on alpha-helix structure and present in hair, nail and wool, or beta keratin, beta-barrel structure, proper of the feather (Voet and Voet, 1995).

Keratin is the third most abundant protein in nature after cellulose and chitin and for its particular structure is highly recalcitrant to the degradation by most proteolytic enzymes (Papadopoulos, 1986).

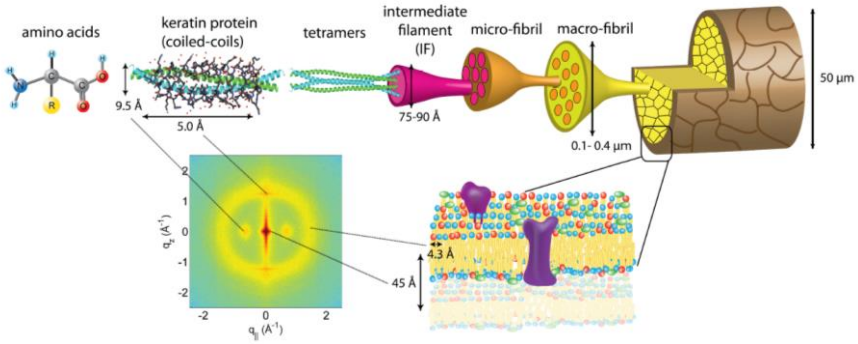

Figure 2- Keratin structure and composition (Yang, *et al.,* 2014).

BASAL MEMBRANE

The basal membrane is the bridge connecting epidermis and dermis. The most abundant component is fibronectin laminin and collagen type IV, VII and XVII, which form the anchoring fibrils and filament respectively. Fibronectin and laminin are glycoproteins involved in network creation and cell adhesion (Breitkreutz, *et al.,* 2013).

DERMIS

The dermis, located below the basal membrane, is formed by connective tissue based on extracellular matrix components like collagen, elastin fiber glycoprotein and proteoglycans. The main types of collagen are type I and II (85-90%), and type II and type V. The collagen is formed in fibrils arranged in quarters strongly cemented together by proteoglycans and hyaluronic acid to form fibers, that turn into fiber bundles (Uitto, *et al.,* 1989). The upper layer of dermis called grain layer present a higher content of elastin, which provides elasticity (Wells, *et al.,* 2016).

Glycosaminoglycans (GAGs) are high molecular weight linear carbohydrates, such as hyaluronic acid, dermatan and chondroitin sulfate. The dermatan sulfate in particular is removed during liming and dehairing process and causes a structural fiber opening (Valeika, *et al.,* 2009).

Proteoglycans are extracellular proteins bound to GAGs, the most present is dechorin which is formed by a polypeptide chain linked to dermatan sulfate. The removal of PGs is important for the process helping in softness and flexibility (Ramos and Liu, 2010).

The hair is firmly anchored in the dermis with hair follicles, formed by proteinaceous fiber of alpha-keratin chain. The hair is composed as follow (Popescu and Hocker, 2007; Yang and Cotsarelis, 2010):

- The bulb, where proliferation and differentiation of cells happen

- The pre keratinized zone, where the disulfide bridges are created.

- The cuticle is the outer surface of the hair, made by a compact structure of alpha-keratin and sheet-like cells which overlay each other.

- The cortex- is the inner structure of hair, made by hard keratin but presenting fewer disulfide bridges and with a more fibrous structure.

- The medulla- is the central structure of hair, not made by keratin but containing different proteins such as citrulline-containing proteins.

Hides delivered to tanneries present yet a subcutis layer named flesh, composed of muscle and fat, and this layer has to be removed as early as possible, usually through mechanical operation, because it can create a barrier to the penetration of chemicals and enzymes.

Although mammals present common composition of skin structure, in the dermis layer some differences can arise based on thickness, angle of weaves of collagen, hair distribution pattern and root depth. These differences must be taken into consideration during the tanning process (Frank, *et al.*, 2006). Considering that skin has to play different functions, there are different stresses area, so skin is a so-called anisotropic material. It is possible to define 3 areas: the butt, up to half from the

backbone to the belly, where fibers are consistent and the skin is firm and stiff, the bellies at the side of the butt are the thinnest parts with open and weak structure and the neck region which is the thickest part but with an open structure (Covington, 2008).

TANNING PROCESS

Tanning is the process able convert and transforms a raw material derived from slaughterhouse, such as hides, into a durable, useful and precious material that is known as leather.

The process of tanning is considered one of the most traditional industrial processes, which has its roots in XX sec., where it was common to use to transform hides into leather and avoid the deterioration of a biological matrix. Untreated skins are susceptible to bacterial degradation and are subjected to putrefaction, but if they are treated to prevent the degradation they can be transformed into more valuable material.

Italian tanneries are recognized worldwide for the final quality of the products. In 2019, Italian districts of leather produced 4.6 billion euros of value, 116 million of m2 of finished leather, with 1180 factories and 17500 employees. Italian production accounts for 65% of all European production and 23% of all worldwide production (Unic, 2019).

The first part of the process (Figure 3), named *beamhouse*, has the crucial role of preparing the hide for the tanning step. Raw hides come from the slaughterhouse mainly fresh (conserved at 4°C for few hours or very few days) or dried (conserved under salt, many days after the slaughter). In both cases, raw hides have to be rehydrated, purified of components not necessary for the tanning and the fiber structure needs to be opened until the fibril bundles.

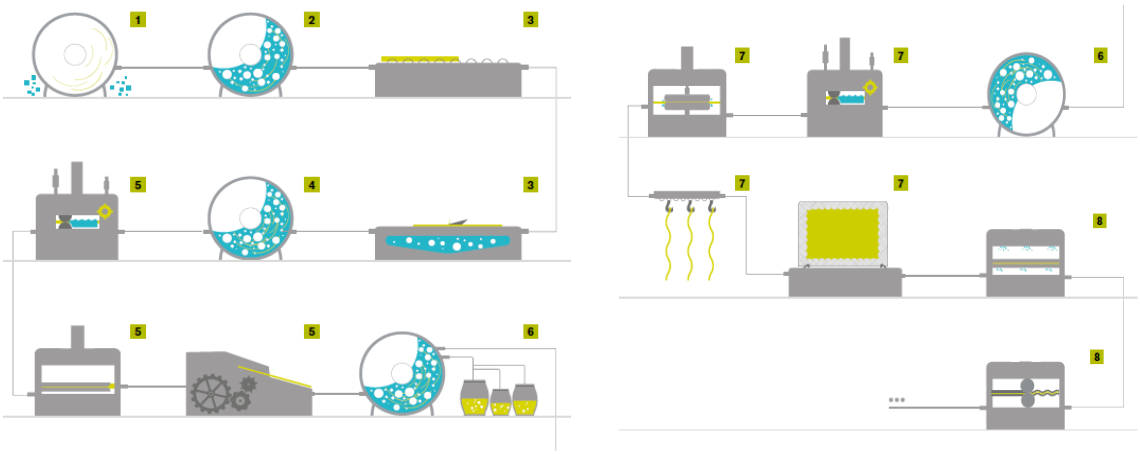

Figure 3- leather tanning process: 1-3 beamhouse operations, 4-6 tanning operation, 7-8 drying and finishing operations **(Dani spa, 2019)**.

The soaking, the first step of beamhouse, is carried out in big drums that contain hides, water and chemical products. The purposes are to rehydrate and fill up the structure to ensure that every component is wet enough to facilitate the movement of dissolved chemical products, to remove the salts in case of dried hides, to remove the dung and dirty material present on the hair and to begin the removal of non-structural components.

Unhairing and liming phases are usually combined because for the traditional process, the removal of hair happens during the liming. While the purpose of unhairing is clear, the liming is carried out traditionally using a lime and calcium hydroxide solution that is combined with sodium sulfide, with the target of unhairing and swelling of the pelt.

Deliming and bating occur together with the presence of deliming agents (carboxylic acids, ammonium salt) to lower the pH, remove the lime and reverse the swelling. Bating leads to the removal of non-structural proteins, hair remnants and pigments via enzymatic action and to the softening of hides.

The last step before tanning is pickling, its purpose is to adjust the collagen to the condition required by the tanning agent. The main chemicals in this step are acids, like formic acid and sulfuric acid.

The strict definition of tanning is the transformation of putrescible organic matter into a stable and durable material, which resists putrefaction. Besides, the tanning has other expected outcomes like the change in appearance (from translucent to opaque), the increase of softness, the release of typical odor and the increase in the denaturation temperature. Eighty percent of the world's output of leather is tanned with Chromium (III), even if alternative tanning agents are emerging and already in use (*e.g.* vegetable tanning). Chrome salts react with ionized carboxyls groups of collagen cementing the structure and avoid the future contact between collagen of the derma and microbial enzymes able to degrade it. The other method is vegetable tanning, where tannins derived from pyrogallols or catechols are used. Tannins bond the phenolic groups of the peptide bonds of the protein chains.

The treatments after tanning have the objective to make the hide softer depending on the final product (upholstery, automotive, fashion) and to mask small defects. They include:

-retanning: to modify the physical properties of leather depending on the final use;

-dyeing: coloring step;

-fatliquoring: useful to prevent fiber sticking when leather is too dry and control the softness

-finishing: meaning the application of polymer films containing colorant and additives to improve the tactile properties of leather-based on the final product.

Every step of the tanning process led to a great amount of pollution, in terms of COD (Chemical Oxygen Demand), sulfur, nitrogen or chrome salts. The beamhouse in particular is responsible for the great part of the pollution load of the wastewater. The discharge has a high content of proteins, sodium chloride, antibacterial agents and presents a high COD, BOD (Biochemical Oxygen Demand), Suspended Solid (Mwinyihija, 2010).

ENZYMES IN TANNERIES

Despite enzymes in tannery are known for over 100 years, it is only in recent years that their use has expanded outside the bating process. The bating process is the only part that already contemplates the use of proteolytic enzymes, but now that biotechnology and biology have better knowledge about enzymes, they could be considered a good solution for future leather (Jayanthi, *et al.,* 2019).

An enzyme is a biocatalyst, which increases the rate of a reaction lowering the activation energy required for the natural route of the reaction. In the active site of the enzyme, the substrate molecule will bind to the enzyme and undergo chemical modification. The binding site between substrate and enzyme is highly specific, is not covalent but based on transient linkages like electrostatic interaction, hydrogen bonding and van der Waals forces. For these reasons, the main factors affecting enzyme activity are temperature and pH.

In bating the used enzymes are proteases, for decades the origin of proteolytic enzymes are pancreatic, those enzymes do not degrade elastin, and are mainly composed of trypsin and chymotrypsin which cleaves peptide link on carbonyl side of basic amino acid of lysine and arginine and with aromatic sidechain respectively. The proteolytic enzymes derived from bacteria are increasing in use due to the low costs. The bacterial enzymes contain also elastolytic activity and are serine protease or metalloprotease (Wanyonyi and Mulaa, 2019).

In the last decade, an increased application of enzymes was registered in the tanning industry, especially for the soaking step. The solubilization of non-collagen components of hide and the open up of the structure is easily performed by enzymes (Saran, *et al.,* 2013). In addition to general proteases for degradation of non-structural protein, the most considered enzymes are (Jianzhong, *et al.,* 2014):

-lipase: cleaving the ester linkages of triglycerides, those enzymes are useful for cleaning the hide surface and solubilize grease in the flesh side allowing chemicals to diffuse better;

-ialuronidase: hyaluronic acid has a bad effect on stiffening the fiber during tanning and avoids the diffusion of chemicals in the section of hide, for this reason, is partially eliminate during soaking;

-amylase: even if starch is absent in hide, it is recognized that application of these glycolytic enzymes helps in opening up the structure attacking other saccharide linkages, such as those present in glycosaminoglycans;

-cellulase or ligninase: are applied to remove the main component of dung allowing the hair shaving and fleshing.

ENZYMES IN DEHAIRING

The traditional reaction that allows the dehairing of hides involves sodium sulfide. The bath derived from the soaking is alkalized using lime or sodium carbonate. At around pH 11 the reducing nucleophilic sulfide ion attacks the disulfide bonds of cysteine. The disulfide bridge is broken and the disulfide group of cystine is reduced to cysteine. The reducing agent acts on softer keratins of the cortex, the pre-keratinized zone and the epidermis. The degradation of the hair proceeds from the tip down to the surface where the rate slows down due to the less surface contact area.

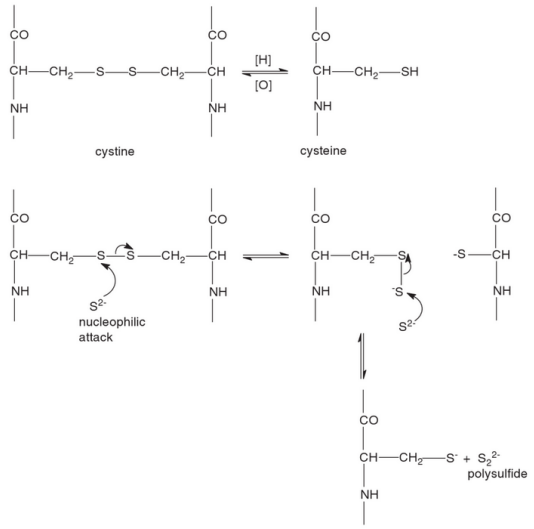

Figure 4- mechanism of chemical dehairing through reducing agent **(Covington, 2008)**.

The hair burning approach ends up with clean and consistent grain, but the hair is partially solubilized in the bath, increasing the COD of the wastewater. Moreover, the wastewater containing polysulfide represents a serious issue, when meshed up with acid wastewater it can generate hydrogen sulfide (H_2S) which is highly toxic.

One of the recently proposed solutions is the conservation of the hair, based on the immunization phenomenon. At a pH superior to 11 the hydroxyl ion attack the methylene group on the cystine and the result is the creation of cysteine and serine, which loses water to form dehydroalanine. The result is that the disulfide bridge became a single sulfur link, more resistant to attack, causing keratin resistance to hair burning. After the so-called "immunization" of hair, the application of a lower dosage of reducing agent is sufficient to obtain the dehairing, avoiding the presence of solubilized hair in the effluent.

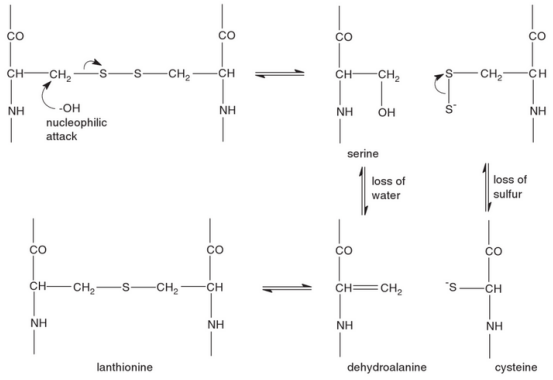

Figure 5- Mechanism of hair saving dehairing **(Covington, 2008).**

Italian tanneries are adopting the hair-saving dehairing approach, even if the downside of reducing agents are the release of hydrogen sulfides in the subsequent stages and the hair, which is pulped in the process increasing the COD.

For these reasons, for decade research groups all around the world, but especially in the nearby of tanneries districts, are focusing on substituting chemical reagents for dehairing with enzymes. The first reported enzymatic dehairing is understudy since 1960 (Beynon and Bod, 1989).

The enzymes explored for the unhairing are basically: low substrate specificity proteases, specific proteases named keratinase, and glycolytic enzymes (Kandasamy, *et al.,* 2012).

The mechanism of action of enzymatic dehairing is not well understood even if the first studies have been published more than 60 years ago. The divergences among the scientific community are related to the enzymatic target during the process: keratin, non-keratinaceous substances, prekeratin zones, etc.

Keratinolytic enzymes, such as keratinase, are reported to break the disulfide linkages and degrade the mature keratin. Yamamura et al. confirmed the importance of reducing the disulfide bridges, testing the combination of a reductase and a protease, both derived from a microorganism (Yamamura*, et al.,* 2002). The degradation of keratin will be counterproductive for hair-saving methods because an excessive attack on the disulfide bridge will lead to the total dissolution of the hair in the bath.

Proteolytic enzymes without keratinolytic activity target the hair bulb and the prekeratinized zones, preserving the outer root and the cuticle and consequently the inner root, even if this hair part is degradable by proteases (Kuntzel and Stirtz, 1958; Ranjithkumar, *et al.,* 2016).

Screening of available proteases revealed that the broad-spectrum proteases (*e.g.* alcalase) are necessary to obtain a complete dehairing while narrow-spectrum enzymes (*e.g*. trypsin) are not effective in dehairing (Yates, 1972).

From histochemical studies conducted to understand the consequences of enzymatic dehairing in the skin matrix, revealed that non-collagenous components are removed when the collagen fibers are opened up. In particular, proteoglycans mucoid substances and hyaluronic acid, essential for the attachment to the basal membrane, are removed resulting in the detachment of hair (Puchtler and Waldrop, 1978).

The role of enzymes that degrade cementing substances thus seems to be crucial, as pointed out by several studies. The main enzymes involved in this process are amylase, hyaluronidase, cathepsin D and lipase.

Based on this data, the dehairing process is a multievent carried out by a blend of enzymes each of them contributing to the detachment of the hair from the bulb. The direct consequence of this in the research is the difficult elaboration of an *in vitro* test of activity. The mainly used tests determine the proteolytic activity relying on casein degradation methods, but casein is not the substrate of other enzymes involved in the dehairing phase so the assay will be not suitable to predict the reaction on skin. Other tests were developed, including keratin azure, based on keratin fibers connected to a chemical dye, dechorin degradation test through chromatographic and immunohistochemical studies, or hide powder, based on pulverized hide linked to a chemical dye. Unfortunately, none of these tests are representative of the complexity of dehairing activity, so a strategy could be to infer all these activities (Gupta, *et al.,* 2002; Jin, *et al.,* 2017).

The advantages of using enzymes are related in first place to the elimination of reducing agents with a consequent reduction in pollution load and increase in the safety of workers. Moreover, the possibility to recover hair that is not degraded could open the way to new strategies of waste revaluation (Wanyoinyi and Mulaa, 2019).

Homogeneous dehairing is the most difficult result to obtain using enzymes because the properties of hides are not uniform. Structural characteristics vary naturally depending on the internal structure of derma and collagen, but other external factors affect the homogeneity of raw hides: the type of hides

(from calf to bull), the geographical provenience (America, Northern Europe) and the season of the year (in winter the hair is thicker and stiffer) (Covington, 2009).

To be economically advantageous over chemical reducing agents, enzymes must be derived from fermentation broth with a limited downstream process. This production system allows having a blend that is desirable because of the broad spectrum of activity on different substrates, but on the other hand can be detrimental for the excessive collagen attack that can impair skin structure and properties (Khandelwal, *et al.,* 2015). The use of recombinant bacterial strains is a solution proposed by many authors, but the costs of production are limiting factors for the application of recombinant enzymatic dehairing. Another defect of many recombinant proteases or keratinases proposed in the literature is the working conditions that are far from the process of tanning. For example, a promising protease derived from *Idiomarina sp. C9-1* was proposed by Zhou et al., but the working conditions of this protease are 60°C and pH of 10.5 (Zhou, *et al.,* 2018). Considering that hide can not be treated over 30°C without damaging the collagen structure, the application of enzymes with high optimum temperature is not possible.

AIM OF THE THESIS

Microbial enzymes have been used for decades in several processes in the industrial, biomedical, environmental, and agro-food sectors. Recent advances in molecular biotechnology, in particular the availability of a vast amount of “omic” data, have considerably increased our understanding of microbial physiology and how microbial cell factories can be implemented to increase the accuracy, safety and efficiency of such processes. The current dehairing process involves chemical compounds such as sulfur/sulfide and lime, which cause safety risks for workers and environmental pollution. In particular, wastewaters present high levels of biochemical oxygen demand (BOD), chemical oxygen demand (COD) and total dissolved solids (TDS), requiring a complex and expensive depollution process.

Microbial enzymes are a good candidate to replace chemicals in the tanning industry because of their high efficiency and low environmental impact. Recent publications have established that for complete dehairing the combination of different enzymes is essential. Enzymes important in this phase seem to be proteases that cleave peptidic bonds of keratin, reductases that disrupt keratin disulfide bridges and saccharolytic enzymes that degrade glycosaminoglycans of the basal membrane of the epidermis.

This project is aimed at the development of a microbially-driven process for hair removal based on secreted enzymes. The first phase of the project consisted of the isolation of microorganisms naturally present on raw hides (cow skin) and displaying specific secreted enzymatic activities. The characterization of this collection has been carried out using a multidisciplinary approach (genomic, proteomic, pilot scale studies) and the most promising isolate was selected. The last part consists of the scale-up of the process, both for bacterial growth and dehairing activity.

MATERIALS AND METHODS

REAGENTS, SUBSTRATES AND GROWTH MEDIA

The hide for sampling were supplied by DANI spa tannery (Arzignano, Vicenza). Various substrates and reagents, such as condensed milk, azocasein, azocoll, keratin azure, Folin Ciocalteau reagent, were purchased by Sigma Aldrich. The growth media used in this paper are: Nutrient Agar 1(NA, Sigma Aldrich), Nutrient Broth (NB, Sigma Aldrich), Feather minimal Medium (FMM, 0.5 g/L NaCl, 0.4 g/L K_2HPO_4, 0.3 g/L KH_2PO_4 and 10 g/L feather), Wool Minimal Medium (WMM, 0.5 g/L NaCl, 0.4 g/L K_2HPO_4, 0.3 g/L KH_2PO_4 and 10 g/L wool) and Feather meal minimal medium (F3M,0.5 g/L NaCl, 0.4 g/L K_2HPO_4, 0.3 g/L KH_2PO_4 and 10 g/L feather meal). The keratin substrates (feather and wool) were supplied by Istituto Zoo Profilattico of Trento.

SAMPLING, ISOLATION, AND PRIMARY SCREENING

Sampling was performed directly on hides presenting dehaired zones at their delivery into tanneries, these zones were larger than 10 cm^2 and are probably due to bad conservation of the hides. The samples were plated in NA and grown for 24, 48 and 72 h at 30°C and 37°C. To enlarge the collection of isolates a sampling was performed also from the working bath of tanneries, 100 ul were plated on NA and grown in the same conditions as above. Various bacterial strains were isolated based on different colony morphologies (color, margin, elevation and texture) and were grown 48h at 30°C on NA plates.

Primary screening was carried out using the Skim Milk Agar Assay. The NA rich medium was supplemented with a solution at 5% (w/v) of condensed milk, resulting in an opaque medium. The degradation halo created by the putative secreted protease was measured in millimeters; the size of the halo is directly proportional to the amount of protease released by the bacterial strain. Further screening was conducted for evaluating the capacity of the microorganisms to grow on minimal media, to maintain the production costs low for a potential scale-up process (Iglesias, *et al.,* 2017). The

minimal medium used were FMM, WMM. The screening was carried out by inoculating the bacterial strains with the minimal culture media and incubating them at 27°C and 30°C overnight, stirring at 160 rpm and monitoring the growth through bacterial colonies count.

GENOME SEQUENCING

The strains that passed the primary screenings were subjected to genome sequencing, using an Illumina MiSeq platform and the kit Nextera XT Illumina (Caporaso, *et al.,* 2012).

The protocol for preparation of the DNA libraries of the samples for sequencing consists of 4 steps:

1) Tagmentation, or the step of fragmentation of the DNA filaments into fragments of about 300 base pairs;

2) Amplification, or a classical PCR reaction for increasing the number of fragments;

3) Purification of the product obtained in the amplification step by 25 removing non-specific reaction products;

4) Quantification of the library obtained and quality control thereof.

The reads obtained were assembled using A5 pipeline and the annotation of the scaffold was performed using RASTk, SpeciesFinder and SignalIP (Coil, *et al.,* 2015; Brettin, *et al.,* 2015; Larsen*, et al.,* 2014; Nielsen, *et al.,* 1997).

SECONDARY SCREENING: ENZYMATIC ACTIVITIES

For the secondary screening a set of enzymatic activity were tested *in vitro*. Each in-vitro experiment was carried out in triplicate.

a) PROTEOLYTIC ACTIVITY

The proteolytic activity was measured in three different tests.

a1) Skim Milk Agar Plate assay

5 µl of supernatant, centrifuged (10 000 g, 15 minutes, 4°C) and filtered, was deposited on a plate of NA medium 10 containing a 3% (w/v) solution of skim milk (Sigma Aldrich). The plates were incubated for 24 hours at 30°C and then the millimeters (mm) of halo present were measured (adapted from Rajamani and Hilda, 1987).

a2) Assay with Azocasein (Sigma Aldrich)

400 µl of azocasein (20 mg/ml solution) was incubated with 400 µl of 15 centrifuged (10 000 g, 15 minutes, 4°C) and filtered supernatant. Incubation took place overnight at 30°C, with stirring (160 rpm). Then 800 µl of 5% trichloroacetic acid (TCA, Sigma Aldrich) was added and the samples were centrifuged (10 000 g, 3 minutes, 4°C). Readings of the value of absorbance (400 nm) were taken. For the control samples (blanks), incubation overnight was carried out only with the azocasein solution and the supernatant was only added after blocking the reaction with TCA. (adapted from Lopes, *et al.*, 2011).

a3) Assay with casein and Folin Ciocalteau reagent (FC reagent)

This assay used 2 ml of centrifuged (10 000 g, 15 minutes, 4°C) and filtered supernatant, incubated for 10 minutes at 37°C, with stirring at 160 rpm with 4 ml of casein solution (5% w/v). After the incubation time, 1 ml of 5% TCA is added to the reaction and incubation is continued for 30 minutes at 37°C, with stirring at 160 rpm. Next, it is centrifuged for 5 minutes at 10 000 g at 4°C. 2 ml of the supernatant thus obtained is added to 5 ml of $NaCO_3$ and 1 ml of F-C reagent, as in the Folin Ciocalteau protocol (adapted from Folin and Ciocalteau, 1929). Incubation of 30 minutes at 37°C, with stirring at 160 rpm, is followed by reading of the absorbance at 660 nm. The blanks are treated as the normal samples but the supernatant is added to the reaction only after the TCA. The absorbance reading was compared to a standard curve obtained with known concentrations of tyrosine.

b) KERATINOLYTIC ACTIVITY

The keratinolytic activity was evaluated using a keratin substrate conjugated with a dye, Keratin Azure (KA). In detail, 1 ml of centrifuged (10 000 g, 15 minutes at 4°C) and filtered supernatant is aliquoted into an Eppendorf tube containing 5 mg of KA. After incubation overnight at 30°C, with stirring at 160 rpm and centrifugation (10 000 g, 3 minutes, room temperature), the absorbance at 595 nm 15 was recorded. The supernatant without any addition was used as a blank to avoid the intrinsic color of each supernatant altering the spectrophotometric reading (adapted from, Wainwright,1982).

c) REDUCTASE ACTIVITY

The reductase activity was evaluated using a reagent conjugated 20 with a dye, DTNB (Sigma Aldrich). In detail, 1 ml of centrifuged (10 000 g, 15 minutes at 4°C) and filtered supernatant is aliquoted into an Eppendorf tube containing 10 mg of feathers and 1 ml of buffer at pH 8. After incubation overnight at 30°C at 160 rpm and centrifugation (10 000 g, 3 minutes, room temperature), 1 ml of DTNB (4 mg/ml) is 25 added. The absorbance at 412 nm was recorded. The absorbance reading was compared to a standard curve obtained with known concentrations of cysteine (adapted from Ellman,1959).

d) ALPHA-AMYLOLYTIC ACTIVITY

1 ml of centrifuged (10 000 g, 15 minutes at 4°C) and filtered supernatant is aliquoted into an Eppendorf tube containing 1 ml of a solution of maize starch. After incubation for 3 minutes at 20°C at 160 rpm, 1 ml of Colour Solution (Sigma Aldrich) is added and it is boiled for 15 minutes. After boiling, it is cooled in ice and 9 ml of H_2O is added. The absorbance at 540 nm was recorded. The absorbance reading was compared to a standard curve obtained with known concentrations of maltose (adapted from Bernfeld, 1955).

e) COLLAGENOLYTIC ACTIVITY

The collagenolytic activity was evaluated using a substrate of collagen conjugated with a dye, Azocol. In detail, 1 ml of centrifuged (10 000 g, 15 minutes at 4°C) and filtered supernatant is aliquoted into an Eppendorf tube containing 1.5 mg of Azocol. After incubation overnight at 30°C at 160 rpm and centrifugation (10 000 g, 3 minutes, room temperature), the absorbance at 516 nm was recorded. The

supernatant "as such" was used as a blank to avoid the intrinsic colour of each supernatant altering the spectrophotometric reading. (adapted from Chavira, *et al.,* 1984).

DEHAIRING ASSAYS (LABORATORY SCALE, PILOT SCALE, INDUSTRIAL TRIAL)

To verify the dehairing activity of the bacterial supernatants, laboratory-scale tests were carried out using rotating jars (Figure 6A), an industrial prototype that reproduces on a small scale the preliminary steps in the tanning of hides. The main difference between the trials consisted in the weight of the hides: 100 gr in the laboratory scale, 5-8 kg in the pilot-scale and 80-100 in the industrial scale.

Each test required about 48 h and 100 g per jar of salted bovine hide, in pieces of about 10x10 cm and 200 ml of water. All tests were carried out using pieces of bovine hide derived from the same animal and followed the protocol given in Table 1.

The pilot-scale and the industrial trials were performed with the same protocol reported in Table 1, but using a little drum and a 1-meter drum respectively (Figure 6B and 6C). The percentages in Table 1 are related to the raw hide weight and the product cited are commercial products specific for the beamhouse (Biodermol Ambiente, Italy).

A C B

Figure 6- A. Rotating Jars; B small drum; C 1m Diameter drum

SOAKING (T=25°C)

w/w relative to the skin	Composition of the bath	Conditions
150%	Water (t=25°C)	Rotation for 60 min, then removal of the treatment bath
0,2%	Sodium carbonate	
0,2%	Biodermol PRODEFAT (bioemulsifier)	
150%	Water (t= 25°C)	Rotation for 60 min, then removal of the treatment bath
0,2%	Sodium carbonate	
0,2%	Biodermol PRODEFAT (bioemulsifier)	
100%	Water (t=27°C)	Rotation for 180 minutes, then rotation for 5 minutes and 55 minutes stopped, for a total of 12 hours.
0,2%	Biodermol TP	
0,3%	Biodermol LIPOL T1/T2S (lipase)	
1,2%	Biodermol WPM (soaking enzymes)	
100%	Water (t=27°C)	Rotation for 12 hours
50%	Supernatant derived from the growth of bacterial strains, containing enzymatic blend	

LIMING (T=27°C)

Gradually increase the pH of the solution with caustic soda (solution 30% w/v).

w/w relative to the skin	Composition of the bath	Conditions
2 %	Lime	Rotation for 60 minutes
1%	Biodermol TP	
1 %	Lime	Rotation for 12 hours
50%	Water (T=27°C)	
0,5%-3,0%	Caustic soda (solution 30% w/v)	
0,5%- 3,0%	Oxidative agent (only if necessary for further cleaning of the skin)	

Table 1- Protocol for dehairing activity tests (laboratory, pilot and industrial scale)

GROWTH VIA FERMENTATION IN BIOREACTORS

The growths via fermentation were performed at Biosphere Srl (Bertinoro, Cesena) using a Solaris, Jupiter 6L bioreactor and Sartorius Biostat D bioreactor for the 5 and 150 liters cultures, respectively. Each test of fermentation was conducted using different growth parameters (temperature, pH, speed of rotation, percentage of inoculum and medium), reported in Table 2, to find the most promising growth condition for the scale-up process (Gupta, *et al.,* 2002; Deroit, *et al.,* 2013). At the end of each fermentation step, the supernatant was tested for proteolytic activity and dehairing activity on samples of skin, following the previously described method.

Trial	*Parameters*				
	T (°C)	*pH*	*Speed (rpm)*	*Medium*	*Inoculum*
1	33	7,3	700	NB	1%
2	30	6,8	700	F3M	1%
3	30	6,8	700	F3M +5g/l feather meal	1%
4	30	6,8	300	F3M +5g/l feather meal	3%
5	30	6,8	300	F3M+ 5 g/l feather meal + 10g/l soy meal	3%
6	37	6,8	500	F3M	1%
7	30	8,4	300-500	F3M	1%
8	30	6,8	700	F3M	1%

Table 2- growth parameters used for the growth via fermentation in bioreactors.

SECRETOME ANALYSIS

The secretome analysis was performed in the laboratory of Prof. Gaspari (Biotecnomed scarl, Catanzaro).

SAMPLE PROCESSING

Two aliquots of 200 μL for each sample were processed by the Filter-Aided Sample Preparation (FASP) method (Wisniewski et al, Nat Methods 2009). Briefly, samples were loaded onto 10 kDa Mw-cutoff centrifugal filter units (Millipore) and spun for 15 min at 14,000 rcf at RT. All centrifugation steps were performed at the same speed and temperature, unless specified otherwise. An aliquot of 200 μL of 8 M urea / 100 mM tris pH 8.0 (urea solution) was added, and filters were spun for additional 15 min (this wash step was repeated a second time). After this first buffer-exchange step, 50 μL of 200 mM iodoacetamide was added to the filters, and spun at 6000 rcf for 30 min. After two wash steps of urea solution (200 μL each) and two wash steps of 50 mM triethyl ammonium bicarbonate buffer (TEAB), 200 ng of proteomics grade trypsin (Sigma) and 60 μL of fresh 50 mM TEAB buffer were added to the filters. Samples were incubated overnight at 37 °C.

The following day, 140 μL of HPLC water were added to the filters. Tryptic peptides were then recovered by centrifugation of the digest mixture (approx. 200 μL) into a new Eppendorf vial.

Before injection in nanoLC-MS/MS, samples were purified by SCX Stage tips as follows:

Samples (2x100 μL for each sample) were diluted 10-fold in Wash B (80% v/v ACN, 0.5% v/v formic acid in water) and purified using StageTips SCX prepared according to Rappsilber et al. (Nat Prot 2007), using SCX disks (3M, Neuss, Germany). StageTips were initially conditioned with: (i) 40 μL of Wash A (20% v/v ACN, 0.5% v/v formic acid in water), (ii) 40 μL of Wash B. After sample loading, StageTips were washed with 80 μL of Wash B. Tryptic peptides were eluted using 10 μL of 500 mM ammonium acetate, 20% acetonitrile. The eluates were dried using vacuum centrifugation, then resuspended in 20 μL of mobile phase A (see below).

NanoLC-MS/MS

Chromatography was performed on an Easy LC 1000 nanoscale liquid chromatography (nanoLC) system (Thermo Fisher Scientific). The analytical nanoLC column was a pulled fused silica capillary, 75 µm i.d., in-house packed to a length of 12 cm with 3 µm C18 silica particles (Dr. Maisch GmbH). Peptide mixtures were loaded directly onto the analytical column. A binary gradient was used for peptide elution. Mobile phase A was 0.1% formic acid, 2% acetonitrile, whereas mobile phase B was 0.1% formic acid, 80% acetonitrile. Gradient elution was achieved at 300 nL/min flow rate, and ramped from 6% B to 42% B in 60 min, and from 35% B to 100% B in additional 8 min; after 5 min at 100% B, mobile phase composition was finally brought to 0% B in 2 min. MS detection was performed on a quadrupole-orbitrap mass spectrometer Q-Exactive (Thermo Fisher Scientific) operating in positive ion mode, with nanoelectrospray (nESI) potential at 1800 V applied on the column front-end via a tee piece. Data-dependent acquisition was performed using a top-12 method with resolution (FWHM), AGC target and maximum injection time (ms) for full MS and MS/MS of, respectively, 70,000/35,000, 1e6/1e5, 50/120. Mass window for precursor ion isolation was 1.6 m/z, and normalized collision energy was 25. Dynamic exclusion was 15 s.

Injected amounts were 2 µL (corresponding to 20 µL of the original secretome sample solutions), except for sample 9 (6 µL) and 14 (4 µL). Considering that, based on total peptide signal obtained, 100 ng per sample were injected, and estimating a sample loss of 50% during sample processing of such low protein amounts, the concentration of the original protein solutions was estimated to be approximately 10 µg/mL (except for samples 9 and 14).

LC-MS/MS data were searched by using Maxquant software using default parameters. The protein databases were: the corresponding bacterium database (either 2VB, 1Dm8, 1Dm15, 3mA2, T2D3) plus a list of proteins identified in your samples by preliminary injections of the controls (thus proteins originating from the following species: *homo sapiens* (keratins), *bos taurus, gallus gallus, ovis aries).*

RESULTS AND DISCUSSION

ISOLATES COLLECTION

We performed the sampling directly on raw hides, provided by DANI tannery in Arzignano (VI) (Figure 7A). The tanners reported the presence of large dehaired zones in some lots, especially during the summer period. This can be due to a defect in the conservation of raw hides, causing the consequent bacterial attack. Since the conservation method with sodium chloride makes the environment unapt for growth, we speculated that some bacterial strains have evolved special mechanisms of degradation of substrate in order to survive. Basing on the same speculation, we also performed a sampling of the bath derived from the process where raw hides present spontaneous dehairing during the first washes.

After incubation plates presented high-density colonies (Figure 7B) with different shapes, colours and sizes.

The plate derived from sampling the dehaired and the non-dehaired zones presented both high density of colonies, but the first one presented more significant differences in terms of colour, shape and size of colonies. We decided to proceed with isolation from the dehaired zone plates and the bath plates.

The isolation step consisting of the pick up of a single colony and growing on a single plate (Figure 7C), led to a collection of 48 isolates (Table 3).

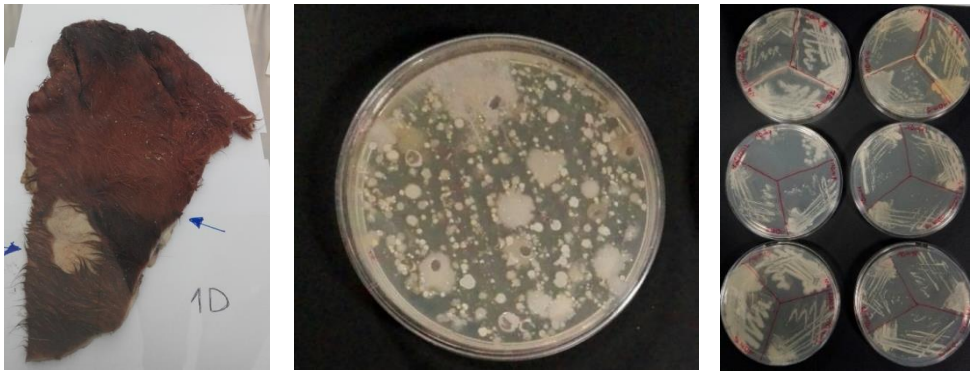

A B C

Figure 7- A: example of hides with a dehaired zone where sampling was performed; B: plate incubation; C: pure isolates plates.

CODE	*TYPE OF SAMPLE*	*SAMPLING*	*ISOLATION*	*COLONIES*		
				shape and size	**colours**	**particular notice**
1Dm2	sampling 1, hide D, dehaired zone	22/01/2018	23/04/2018	convex	white, shiny	mucous
1Dm3	sampling 1, hide D, dehaired zone	22/01/2018	23/04/2018	soft edges	white, opaque	
1Dm4	sampling 1, hide D, dehaired zone	22/01/2018	23/04/2018	small, round, convex	yellow/orange	
1Dm5	sampling 1, hide D, dehaired zone	22/01/2018	23/04/2018	convex	white shiny	mucous
1Dm6	sampling 1, hide D, dehaired zone	22/01/2018	08/05/2018	soft edges	white opaque	
1Dm7	sampling 1, hide D, dehaired zone	22/01/2018	23/04/2018	soft edges	white opaque	
1Dm8	sampling 1, hide D, dehaired zone	22/01/2018	23/04/2018	convex	white shiny	mucous
1Dm14	sampling 1, hide D, dehaired zone	22/01/2018	23/04/2018	soft edges	white opaque	
1Dm15	sampling 1, hide D, dehaired zone	22/01/2018	23/04/2018	convex	white shiny	mucous
2Am1	sampling 2, hide A, dehaired zone	21/02/2018	23/04/2018	small, round, convex	white shiny	
2Am2	sampling 2, hide A, dehaired zone	21/02/2018	23/04/2018	small, round, soft edges	white transparent	
2Am3	sampling 2, hide A, dehaired zone	21/02/2018	23/04/2018	small, round, convex	light yellow shine	
2Am4	sampling 2, hide A, dehaired zone	21/02/2018	08/05/2018	small, round	light yellow shiny	smell
2Am5	sampling 2, hide A, dehaired zone	21/02/2018	23/04/2018	glaze	transparent	
2Am6	sampling 2, hide A, dehaired zone	21/02/2018	23/04/2018	small round, convex	white transparent	

3Am2	sampling 3, hide A, dehaired zone	17/04/2018	23/04/2018	round, half size	white shiny	
3Am3	sampling 3, hide A, dehaired zone	17/04/2018	02/05/2018	small, round	white transparent shiny	
3Am4	sampling 3, hide A, dehaired zone	17/04/2018	09/05/2018	spreading edges	white	
3Am6	sampling 3, hide A, dehaired zone	17/04/2018	09/05/2018	very small round	light yellow shiny	
3Am8	sampling 3, hide A, dehaired zone	17/04/2018	02/05/2018	very small, few	flou yellow	
3Am9	sampling 3, hide A, dehaired zone	17/04/2018	09/05/2018	round	yellow	
3Am10	sampling 3, hide A, dehaired zone	17/04/2018	23/04/2018	small, transparent, soft edges	transparent with white middle	
3Am11	sampling 3, hide A, dehaired zone	17/04/2018	09/05/2018	small, round	white, transparent shiny	
3Bm2	sampling 3, hide B, dehaired zone	17/04/2018	09/05/2018	round, convex	white shiny	migration
3Bm3	sampling 3, hide B, dehaired zone	17/04/2018	09/05/2018	glaze	yellow-white	migration
T1R1	Soaking bath	09/04/2018	13/04/2018	round, defined edges	orange shiny	
T1R2	Soaking bath	09/04/2018	13/04/2018	big, soft edges	white darker middle	
T1R3	Soaking bath	09/04/2018	13/04/2018	round, convex	white shiny	
T1R4	Soaking bath	09/04/2018	13/04/2018	big, round, plate	white opaque	
T2R1	Soaking bath	11/04/2018	13/04/2018	small, convex	orange shiny	
T2R2	Soaking bath	11/04/2018	13/04/2018	small, round	green, translucent	smell
T2R3	Soaking bath	11/04/2018	13/04/2018	small, round	yellow	
T2R4	Soaking bath	11/04/2018	13/04/2018	small, round	green, translucent	smell
T2D1	Dehairing bath	11/04/2018	08/05/2018	small, round	green, translucent	smell
T2D2	Dehairing bath	11/04/2018	08/05/2018	small, round, convex	yellow shiny	
T2D3	Dehairing bath	11/04/2018	07/05/2018	small, convex	strong orange	
T2D4	Dehairing bath	11/04/2018	08/05/2018	small, round, convex	white translucent	
T2D5	Dehairing bath	11/04/2018	08/05/2018	small, round, convex	white shiny	mucous
T2D6	Dehairing bath	11/04/2018	08/05/2018	small round	flou yellow	
T2D7	Dehairing bath	11/04/2018	08/05/2018	round	transparent shiny	
T2D8	Dehairing bath	11/04/2018	08/05/2018	round, small	green, translucent	smell
T2D9	Dehairing bath	11/04/2018	08/05/2018			
T2D10	Dehairing bath	11/04/2018	08/05/2018			
T2D11	Dehairing bath	11/04/2018	08/05/2018			
T2C1	Liming bath	11/04/2018	23/04/2018	small, round, convex	white translucent	
T2C2	Liming bath	11/04/2018	23/04/2018	small, round, convex	white translucent	
T2C3	Liming bath	11/04/2018	23/04/2018	glaze no colonies	transparent	migration
T2C4	Liming bath	11/04/2018	23/04/2018	small, convex	yellow shiny	

Table 3-Isolates derived from the sampling and their characteristics

FIRST SCREENING: SKIM MILK AND MINIMAL MEDIA

Once we have prepared the collection of isolates, it started the screening process. The dehairing activity is a complex result of different enzymatic activity and kinetics, so there is not a unique test in vitro. We decided to perform a first screening selecting bacteria able to secrete enzymes in the external environment, in particular proteases. Bacterial strains able to secrete proteases produce a halo around the colony, the result of the skim milk degradation.

Thirty-five isolates presented a halo after 24 h or 48h of incubation, many of them were unmeasurable at 48h because they were too extended. Other isolates (3Bm2, 3Bm3, T2C3) presented the migration phenomenon, so we were unable to directly quantify the halo dimension.

According to the final use of the enzymatic blend, the tanneries, the costs of production must be taken into account. For this reason, we tried to select since the early stage an isolate able to grow on minimal media at suitable conditions. The 35 isolates with proteolytic secreted activity were grown in two minimal media: FMM (feather) and WMM (Wool). The growth was evaluated by optical density measurements and is reported in Table 4. We have to point out that due to the opaque nature of the minimal media, OD600 measurements can provide only qualitative data. Only 7 isolates were able to grow using the feather as a source of carbon and nitrogen and 7 using wool. 1Dm8, 1Dm15, 3Am4 and T2D3 were able to grow on both media.

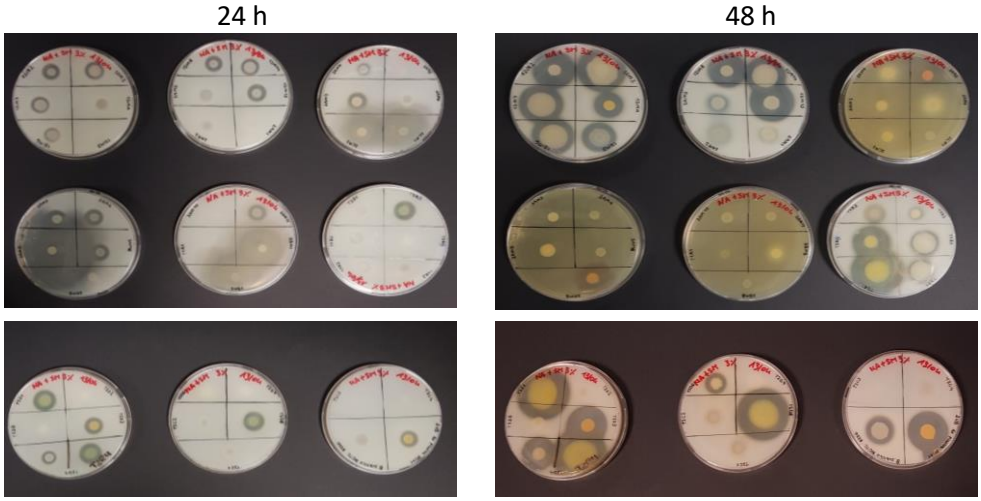

Figure 8- skim milk agar plate at 24h and 48h of incubation.

	SKIM MILK			*MINIMAL MEDIA GROWTH*	
	HALO	DIMENSION (mm) 24 H	DIMENSION (mm) 48 H	FMM	WMM
1Dm2	yes	7	20		
1Dm3	yes	4	10	YES	
1Dm4	yes	1	9		YES
1Dm5	yes	-	8		
1Dm6	yes	2	9		
1Dm7	yes	4	10		
1Dm8	yes	7	17	YES	YES
1Dm14	yes	4	8	YES	
1Dm15	yes	7	21	YES	YES
2Am1	no	-	-		
2Am2	no	-	-		
2Am3	yes	1	1		
2Am4	yes	2	n.d.		
2Am5	yes	-	n.d.		
2Am6	yes	-	n.d.		
3Am2	yes	6	n.d.	YES	
3Am3	yes	7	n.d.		
3Am4	yes	6	n.d.	YES	YES
3Am6	yes	6	n.d.		
3Am8	yes	-	n.d.		
3Am9	yes	58	n.d.		
3Am10	no	-	-		
3Am11	yes	6	n.d.		
3Bm2	yes	28	n.d.		
3Bm3	yes	48	n.d.		
T1R1	yes	-	n.d.		
T1R2	yes	-	2		YES
T1R3	yes	1	2		
T1R4	yes	2	4		
T2R1	yes	-	4		
T2R2	yes	7	25		
T2R3	yes	-	17		
T2R4	yes	7	13		
T2D1	yes	7	16		
T2D2	no	-	-		YES
T2D3	yes	6	20	YES	YES
T2D4	yes	5	10		
T2D5	no	-	-		
T2D6	yes	-	7		
T2D7	no	-	-		
T2D8	yes	6	14		
T2D9	no	-	-		
T2D10	no	-	-		
T2D11	no	-	-		
T2C1	no	-	-		
T2C2	no	-	-		
T2C3	no	-	-		
T2C4	no	-	-		

Table 4- Summary of primary screening: skim milk agar plate and growth on minimal media

The 10 isolates able to grow on minimal media were selected for further characterization, first of all, a Gram staining (Table 5 and Figure 9).

Isolate Name	*Gram Staining*	*Shape of cell*
1Dm3	Positive	Bacilli
1Dm4	Positive	Cocchi
1Dm8	Positive	Bacilli
1Dm14	Positive	Bacilli
1Dm15	Positive	Bacilli
3Am2	Negative	Rod shape
3Am4	Positive	Cocchi
T1R2	Positive	Bacilli
T2D2	Negative	
T2D3	Negative	

Table 5-Gram staining results

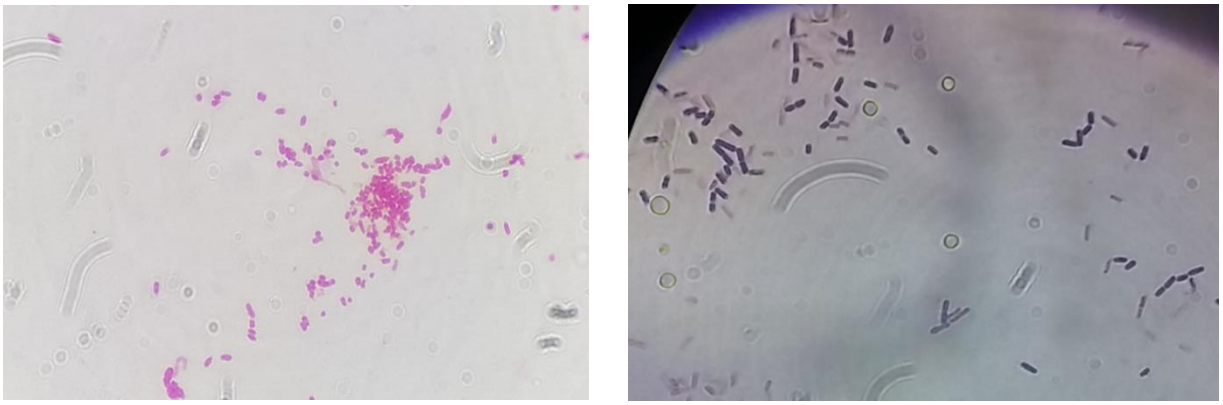

Figure 9- 3Am2 and 1Dm8 at microscope (100x)

SPECIES IDENTIFICATION

After the assembly of the NGS data using A5 pipeline, species identification was performed using SpeciesFInder 1.2 and Kmer, which analyse the 16S. The results obtained are reported in Table 6.

Due to the presence of a potential pathogenic species among the isolates (*Streptococcus aureus*) and considering that a pathogen would be excluded for the industrial application, we performed a check for pathogenicity using PathogenFinder (Cosentino, *et al.,* 2013). None of the 10 isolates resulted as predicted human pathogen.

The assemblies were annotated using a tool kit of RASTK, to assess the number of predicted proteins, while the number of secreted proteins was estimated using the tool SignalP (Armenteros, *et al.,* 2019).

Code	*Isolate*	*Species name*	*Phylum*	*Proteins*	*Protein with signalP*	*% protein with signalp*
Bio1	3Am2	*Aeromonas salmonicida*	g-Proteobacteria	4614	304	6.58
Bio2	3Am4	*Arthrobacter arilaitensis*	Actinobacteria	4672	191	4.08
Bio3	1Dm3	*Bacillus cereus*	Firmicutes	3487	418	11.98
Bio4	1Dm4	*Staphylococcus sciuri*	Firmicutes	6119	103	1.68
Bio5	1Dm8	*Bacillus subtilis*	Firmicutes	2874	275	9.56
Bio6	1Dm14	*Bacillus cereus*	Firmicutes	4241	430	10.13
Bio7	1Dm15	*Bacillus spp.*	Firmicutes	6483	268	4.13
Bio8	T1R2	*Bacillus kochii*	Firmicutes	4285	269	6.27
Bio9	T2D2	*Cronobacter dublinensis*	g-Proteobacteria	5839	408	6.98
Bio10	T2D3	*Chryseobacterium indologenes*	Bacteroidetes	4420	572	12.94

Table 6- Results of genomic identification and protein annotation

To study in deep the data obtained for isolate 1Dm15, which was identifies as general *Bacillus sp*., the identification was confirmed with the ANI index **(Rodriguez and Konstantinidis, 2014)**.

The closest relative identified that we could identify was *Bacillus sp* JS, a plant growth-promoting *rhizobacterium* from Korea **(Song, *et al.*, 2012).**

The second was *Bacillus sp.* MD5, Chinese isolate applied in the food industry **(Gou, *et al.*, 2018)**.

The described species that results closest to the 1Dm15 strain was *B. subtilis*, with an ANI score of 95,6%. This data is approximate for the species level, nevertheless, it is evident that many *Bacillus sp.*, not classified as *B. subtilis*, present a similar ANI index. The *B. licheniformis* and *B. pumilus* species, used as a control in-group and out-group, show that 1Dm15 is similar to the complex "simil-subtilis" (Figure 10).

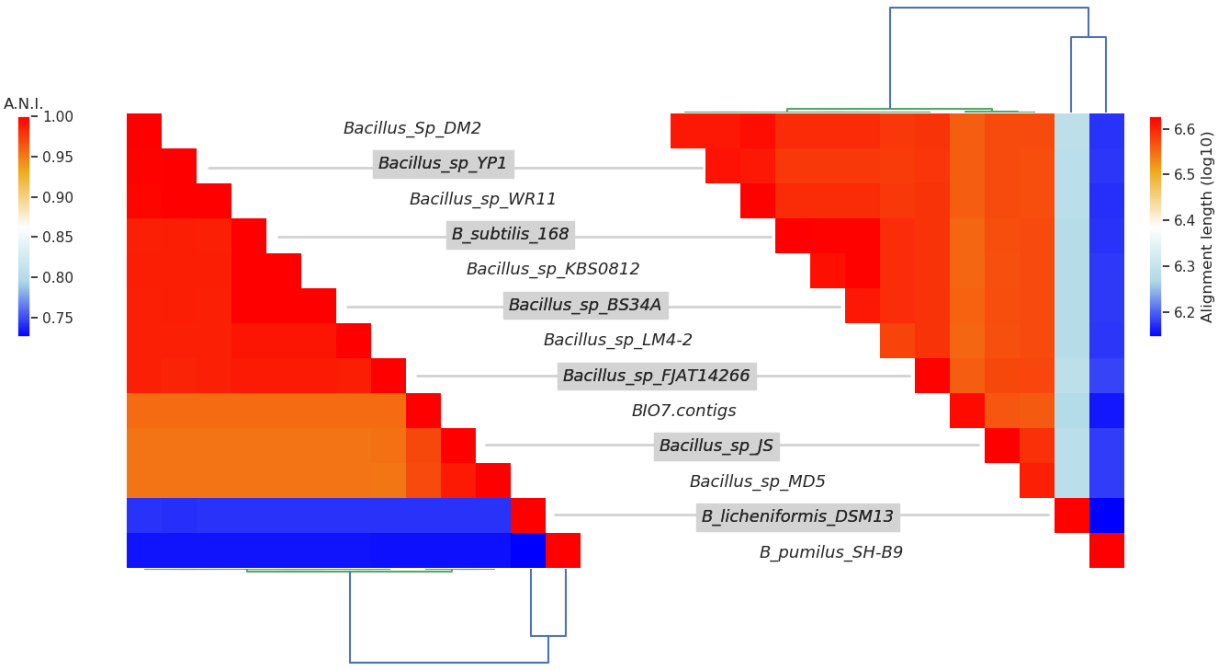

Figure 10- ANI and alignment length values between *Bacillus sp*

SECONDARY SCREENING

According to the literature, some enzymatic activities were selected for further investigations on the 10 isolates. In particular, beyond proteolytic activity, we were interested in the amylolytic activity, which is important for the opening up of the fibers and the disaggregation of epidermidis, keratinolytic activity responsible for the dissolution of keratin, collagenolytic activity that has to be maintained at a low level for the preservation of the dermis and reductase activity involved in the reduction of cysteine bonds. The results showed in Figure 11 indicate that collagenolytic activity is present in all strains except for 1Dm4, 3Am4 and T2D2. Amylolytic activity and reductase activity are present in almost all isolates in all media. Results on keratinolytic activity present high variability in terms of reproducibility, this can be due to the substrate of the test which is not always homogenous and provides poorly replicable results.

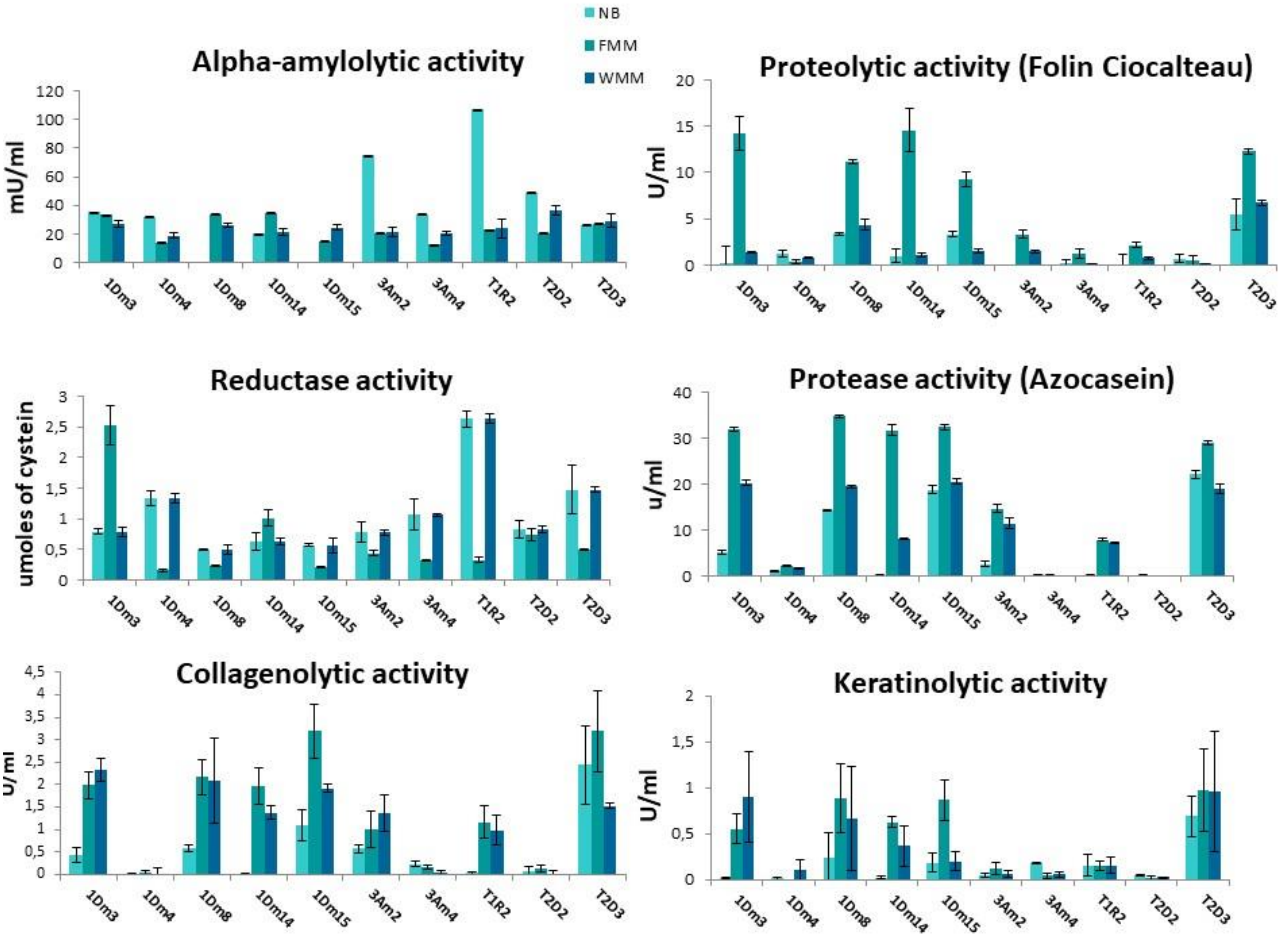

Figure 11- Enzymatic activity performed on supernatant of NB, FMM and WMM of all 10 isolates.

The enzymatic activity tested *in vi*tro needs to be confirmed by the dehairing activity. The supernatant of each strain and media was tested for all the enzymatic activities and it was also challenged in the dehairing test.

The data were collected in a heatmap (Figure 12), where the darkest blue corresponds to a higher activity. Overall, it is possible to appreciate darker blue in the panel of FMM and WMM, thus confirming the ability of minimal media to induce the production of hydrolytic enzymes.

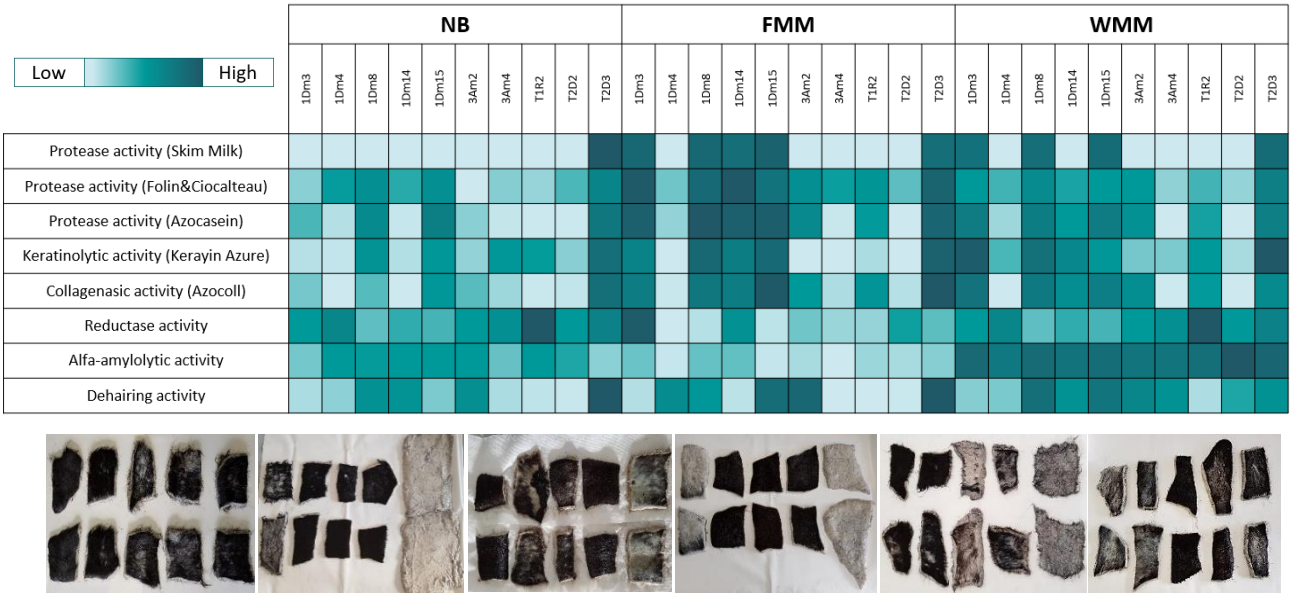

Figure 12- A) heatmap of the enzymatic tests and the dehairing test, B) results obtained on hides.

Surprisingly, some isolates like the 1Dm3 in FMM presented high enzymatic activity but very poor dehairing ability and on the contrary some isolates with lower enzymatic activity 3Am2 in FMM performed very good on raw hides.

The discrepancy between enzymatic activity measured *in vitro* and the *in vivo* test could be explained with the presence of other enzymes important for the process that was not analysed or with the different specificity of enzymes even from the same family. This could be supported by the results

obtained with three different protease assays: they presented not coherent results because of the difference in the assay substrate.

The collagenolytic activity seemed to be present in almost all strains and conditions, which could represent an issue in terms of final results on leather. The correct working conditions, such as the time of interaction between supernatant and hides, have to be established to overcome collagen degradation.

Based on these results, we decided to select 4 isolates for further characterization: 1Dm8, 1Dm15, 3Am2 and T2D3.

Except for T2D3 in NB, the dehairing activity was not provided when isolates were grown in rich media such as NB. It is possible to speculate that the presence of keratin substrate induces the production of different enzymes and that the differences in enzymatic contentment of the supernatant could be indicative of the action in the dehairing process. To confirm that, we performed an SDS-PAGEof of all the supernatant to evaluate the protein pattern on the gel (Figure 13).

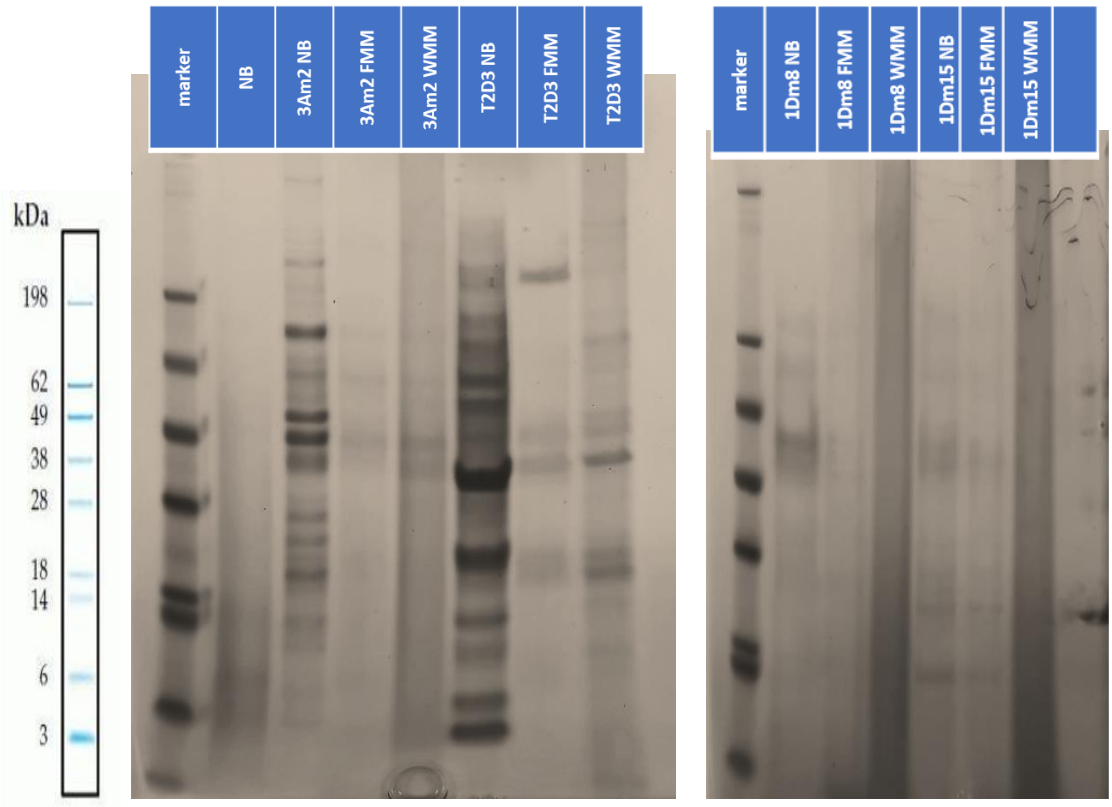

Figure 13- SDS-PAGEof the precipited supernatant of the four isolates grown in different media.

It was not possible to detect significant differences in bands among the same isolate grown in different media, because of the interference of degraded keratin, but it was possible to appreciate a higher concentration of secreted proteins in the NB medium.

SELECTION OF MOST PROMISING ISOLATE

a)PROTEOMIC ANALYSIS

To select the most promising isolate among the 4 selected isolates, we used three strategies:

- analyze the secretome, *i.e.* the complexity of proteins released in the medium by bacteria;
- perform a downstream process, *i.e.* lyophilization;
- perform unhairing test on a pilot scale.

The analysis of the secretome was performed to possibly correlate the presence of some secreted enzymes to the unhairing effect. The analysis revealed that hundreds of proteins were secreted in the medium and that qualitatively the content of the secretome varies on the base of the medium used for the growth.

The total number of detected proteins is reported in Table 7. The sample 3Am2 in WMM returned a very low amount of protein detected, due to a contamination problem. For the 3Am2 and the T2D3 the number of proteins detected was higher in the minimal media, while for 1Dm8 the highest number was present in NB media.

Isolate	*NB*	*FMM*	*WMM*
1Dm8	251	239	217
1Dm15	239	285	175
3Am2	168	237	22
T2D3	146	248	211

Table 7- number of detected proteins

The Venn diagrams (Figure 14) report the number of proteins of the core secretome (*i.e*. the proteins present in all the media) and the minimal media secretome.

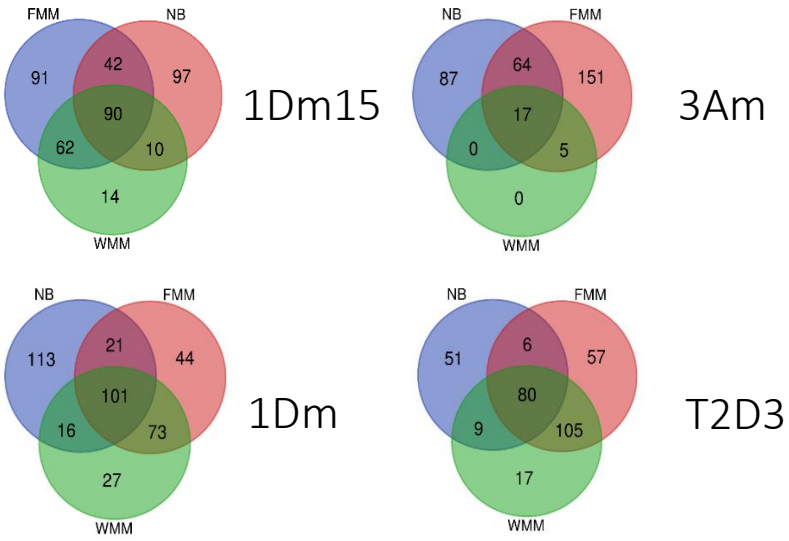

Figure 14- Venn diagrams of proteins shared in the different media.

The protein ID was combined with the identification obtained with RAST during genome analysis. The X-MM secretome, *i.e*. the proteins present only in the minimal medium growth are reported in Tables 8-11 (Appendix).

To have an overview of the degradative potential of the supernatant we calculated the percentage of protease, glycolytic enzymes and lipolytic enzymes within the secretomes. Proteases were the most present among the enzymes of interest accounting for the 3-15% of the total proteins detected. The

T2D3 resulted in a lower amount of enzymes of interest, but this could be due to a more difficult RAST annotation, because *Chriseobacterium* is not so well genetically characterized.

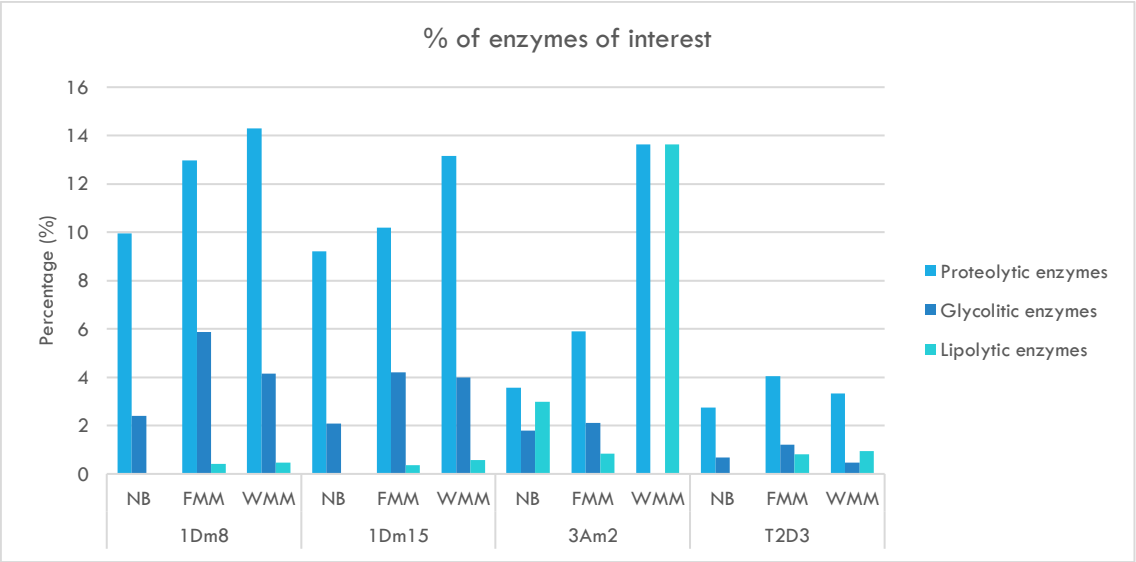

Figure 15-% of enzyme of interest among total protein detected in the secretome

To have an idea of prevalence inside the sample of different proteins, we performed a second analysis on the obtained data. Instead of using the MS/MS count for the semiquantitative analysis, we applied the summed intensities with the software MaxQuant **(Wisniewski, *et al.,* 2014)**. The proteins with a percentage of summed intensities higher than 1% are reported in Tables 12-15.

From the proteomic studies of these 4 isolates, the 1Dm8 and 1Dm15 present the most promising results in terms of the presence of enzymes of interest, *i.e.* proteases, lipases and glycolytic enzymes.

b) SPRAY DRYING TESTS

The downstream process during the fermentative production of enzymes is crucial, so we decided to perform some experiments of spray drying to understand which of our isolates can maintain high enzymatic activity after drying.

The spray drying process was conducted in collaboration with Nanonmia Srl (Zevio, Verona). Different protocols for the spray drying steps were used, the data obtained using the different protocols are reported in table 16, while the media of the data are in table 17.

Considering the media of dry weight and the media of residual activity the 1DM15 and 1Dm8 were the most promising isolates: the dry weight is from 67% to 83% for 1Dm8 and from 52% to 75% for 1Dm15, and the residual activity is over 80% in both isolates.

strains	*dry weight (100 ml, oven)*	*dry weight (100 ml, spray drying)*	*% of residual dry weight*	*proteolytic activity before (U/ml)*	*proteolytic activity after (U/ml)*	*% of residual activity*
1Dm8_1	249	161	67,08	31,77	29,48	92,79
1Dm8_1bis		173	72,08		28,54	89,84
1Dm8_2		198,6	82,75		29,44	92,68
1Dm8_3		200,8	83,33		28,72	90,38
1Dm8_4		164,5	68,54		28,89	90,93
1Dm8_5		187,3	77,91		29,76	93,66
1Dm15_1	224	115	52,27	31,46	28,68	91,17
1Dm15_2		148,37	70,059		27,29	86,75
1Dm15_3		166,8	75,81		25,45	80,91
3Am2_1	171	95	55	25,45	16,74	65,76
3Am2_2		106	62,35		17,5	68,76
3Am2_3		96,4	56,7		19,24	75,58
3Am2_4		59	34,7		17,6	69,17
3Am2_5		43	25,29		17,71	69,58
T2D3_1	255	122	46,92	28,26	24,48	86,61
T2D3_2		135,8	52,23		24,65	87,22
T2D3_3		132,5	47,32		25,35	89,68

Table 16- Data obtained from spray drying, all the isolates were grown in FMM.

	Media of dry weight (%)	*Media of residual activity (%)*
1Dm8	75,28	91,71
1Dm15	66,22	86,28
3Am2	46,81	69,77
T2D3	48,82	87,84

Table 17- media of the data obtained in different protocols.

c)DEHAIRING PILOT SCALE TESTS

The third strategy applied for the selection of the most suitable isolate was the pilot-scale tests of dehairing.

Upscaling the process from 200 gr of raw hides to 8-10 kg, required an consistent number of tests for the setting of the parameters (reported in Table 18). The beamhouse phase varies in function of the type of raw hides and presents well-defined stages. Because of the chemistry of the reaction, the traditional liming includes both the unhairing step and the addition of lime. In the case of enzymatic dehairing it is necessary to dedicate a specific phase to the dehairing without the interference of other chemicals.

We conducted some tests for the setting of the conditions, then we performed a triplicate of dehairing tests for each of the strains grown in FMM. The condition setting was performed varying the recipe of the soaking (in terms of time, pH, temperature and chemicals added), the other component of the beamhouse (sodium carbonate, lime, etc.) but also the working conditions (time of contact between supernatant and hides, pH or temperature).

n. test	*Date of test*	*Product used*	*Results*
1	21/05/2018	Control strain supernatant	unhairing is observed but still hair zones are present
2	28/05/2018	Control strain supernatant	no unhairing, improvement after the addition of liming
3	04/06/2018	Control strain supernatant	Complete unhairing, small hair remained in the bulb, epidermidis not completely removed.
4	29/01/2019	1Dm15	Unhairing complete, addition of 0,6% of reducing agent to clean the grain, no epidermidis, persistent odour
5	04/02/2019	3Am2	Unhairing complete, addition of 0,4% of reducing agent to clean the grain, no epidermidis
6	12/02/2019	1Dm8	No unhairing, consistent amount of fat, 0,6% of sulphide used suspended test
7	18/02/2019	1Dm8	Unhairing complete, addition of 0,6% of sulphide, no epidermidis, little zone of not removed hair
8	25/02/2019	T2D3	Unhairing complete, addition of 0,6% of sulphide, no epidermidis, little zone of not removed hair, slightly bacterial attack to the grain
9	11/03/2019	3Am2	Unhairing complete, strong attack to the collagen and to the grain, suspended test
10	02/04/2019	3Am2	No unhairing, hardened hide, suspended test
11	09/04/2019	3Am2	Unhairing present, but problems with pH control, suspended tests
12	15/04/2019	1Dm15	Unhairing complete, green fleshing, very small amount of residual hair, completed with oxidative liming
13	21/04/2019	1Dm15	No unhairing, hair well attached, presence of fat on surface, hardness of hide, suspended test
14	03/06/2019	1Dm15	Unhairing complete, started early than usual, completed with oxidative liming, some visible hair

15	11/06/2019	1Dm15	Unhairing complete, completed with oxidative liming
16	18/06/2019	1Dm15	Unhairing complete, completed with oxidative liming, but presence of bacterial attack to the grain
17	25/06/2019	1Dm8	Unhairing partially complete, but the bacterial attack to the grain is extremely wide.
18	02/07/2019	1Dm8	Unhairing complete, completed with oxidative liming
19	10/07/2019	T2D3	Hide was digested by the enzymatic preparation, odour of fermentation, absence of bath, suspended test
20	16/07/2019	3Am2	Hide was partially digested, hair intact, suspended test
21	23/07/2019	3Am2	3Am2Unhairing complete, completed with oxidative liming

Table 18- Summary of the dehairing test performed at a pilot scale level.

Several issues were encountered during the test, first of all, the variability among the hides that are treated. Colour of hair, presence of fat, geographical provenience and class weight led to results difficult to compare and force to change the recipe ongoing to adjust the condition of the test. Moreover, the chance to perform a single test per time prevented the possibility to have a positive or negative control helping in interpreting the results.

The overall conclusion of this part of the tests was that the supernatant of all isolates has good dehairing ability (Table 19), comparing the number of positive results with the negative the most promising isolates were 1Dm15 and 1Dm8 (Table 20).

	% positive test	*% negative test*
1Dm8	66,7	33,3
1Dm15	60,0	40,0
3Am2	50,0	50,0
T2D3	33,3	66,7

Table 20- percentage of positive results

Strain	*Results*
1Dm15	 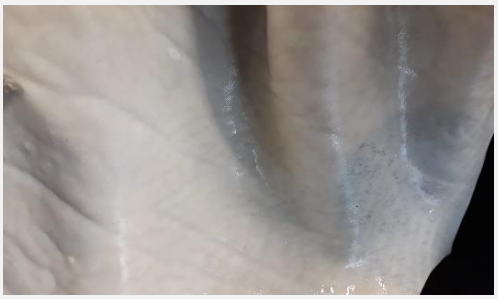 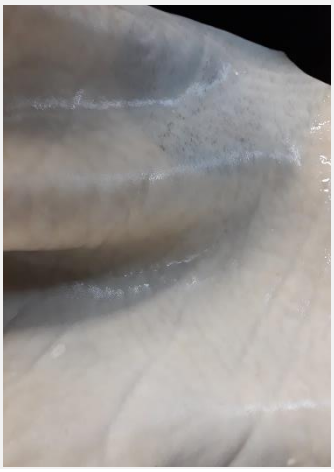  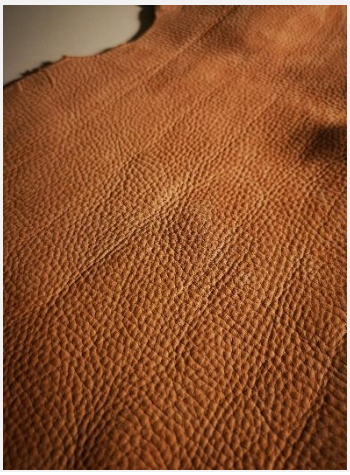
1Dm8	   

3Am2	 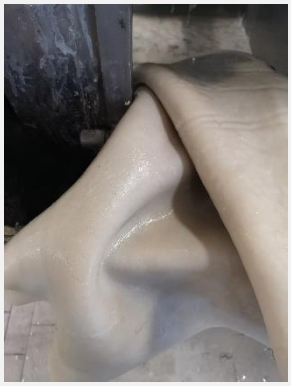 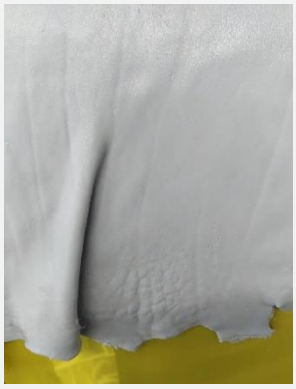 
T2D3	  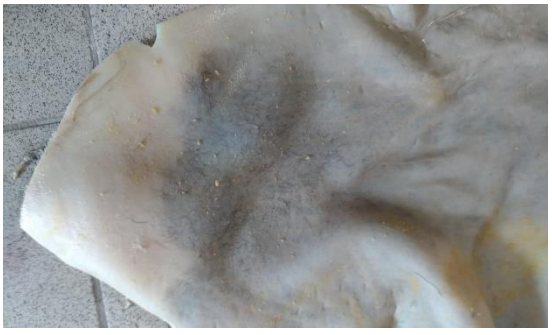 

Table 20- results obtained in the pilot scale dehairing test

Since results in the unhairing tests with 1Dm15 are more stable, that 1Dm8 and 1Dm15 are very similar, also at a genetically level, and that 1Dm15 seems to grow stronger on FMM, we decided to continue the characterization with 1Dm15 *Bacillus spp*.

BIOREACTOR GROWTH

To understand the possibility to scale up the process, we decided to grow the strain in bioreactors.

First trials were performed in the lab with a 1-L bioreactor (Sartorius). The growth in bioreactor compared with the one performed in the Erlenmeyer flask showed an increase in the growth of the cells (OD600) but also in the proteolytic activity, which is chosen as the general test to follow the enzymatic expression in the supernatant (Figure 20). In particular, the azocasein test revealed that after 8 hours of growth the proteolytic activity doubled.

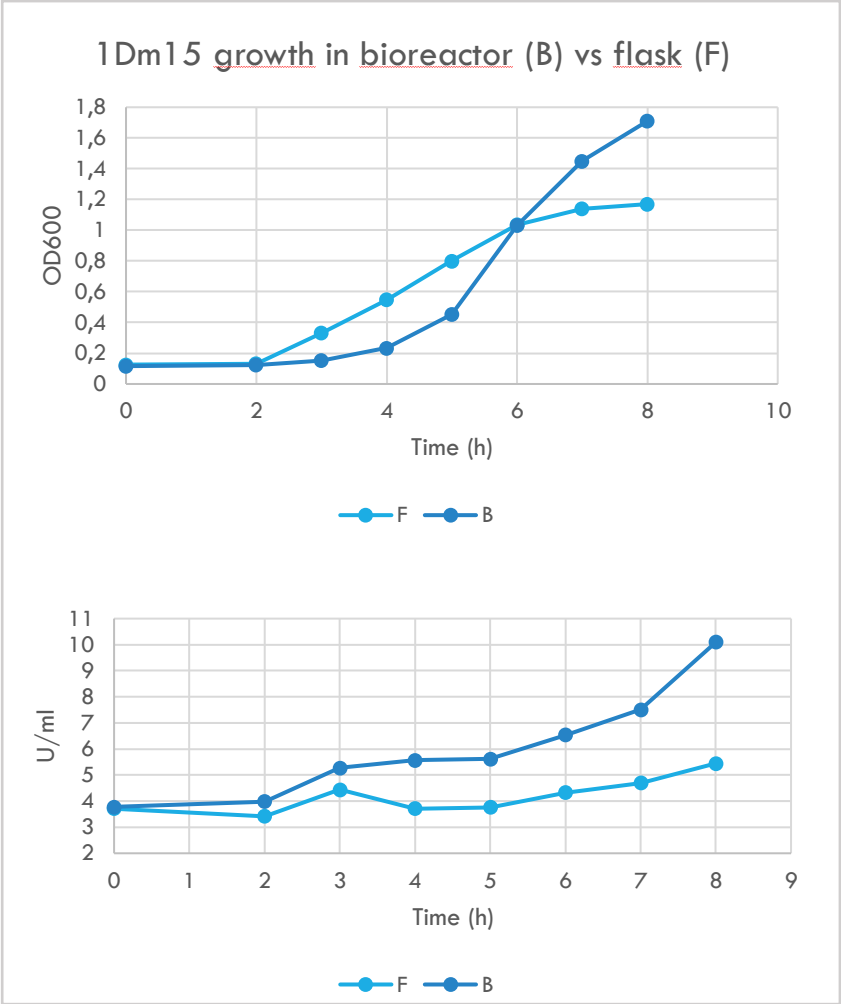

Figure 20- Compared growth and proteolytic activity in Erlenmeyer flask (F) and bioreactor (B).

These experiments were performed at Biosphere Srl (Bertinoro, FC) to understand the parameters that optimize the growth and the yield in terms of enzymatic activity of the supernatant.

The isolate 1Dm15 was grown with different parameters: temperature, pH, speed of agitation, growth media and percentage of inoculum (reported in Table 21). During each test, we verified the cell growth using viable cell count, the proteolytic activity with skim milk agar plate and azocasein. At the end of each test, an aliquot of the supernatant was conserved for further proteomic analysis and the rest tested on dehairing tests.

Tests	*Parameters*				
	Temperature (°C)	*pH*	*Speed*	*Growth media*	*Inoculum*
BDL.20.01	30	7,3	700	NB	1%
BDL.20.02	30	6,8	700	F3M	1%
BDL.20.03	30	6,8	700	F3M +5g/l	1%
BDL.20.04	30	6,8	300	F3M +5g/l	3%
BDL.20.05	30	6,8	300	F3M+ 10g/l soy meal	3%
BDL.20.06	37	6,8	500	F3M	1%
BDL.20.07	30	8,4	300-500	F3M	1%

Table 21- Growth parameters of the different trials in 5-L bioreactor.

The growth on rich media, as confirmed in Figure 21, limited the expression of hydrolytic enzymes, like proteases, the bacteria have free access to all the reedy to use nutritional elements in the media without the necessity to degrade more complex substrates. Consequently, the registered proteolytic activity was very low. Changing the media with a minimal medium containing only keratin as a source of carbon and nitrogen the strain was forced to secrete hydrolytic enzymes, form test BDL.20.02 to test BDL.20.07.

Increasing the amount of keratinaceous substrate (feather meal) the secretion of protease increased to the maximum with activity at 24 h of 10.7U/ml (test BDL.20.03). Also adding to the F3M the soy meal, increased the general proteolytic activity, probably due to the fact the strain grows better, as was demonstrated by the cell growth count at the end of the fermentation (Figure 21, panel B). In the test BDL.20.03-04-05, where it was present additions in the minimal media, the CFU/ml reached at the end of the growth are of one order higher than the other tests, as it was for the growth on rich media, BDL.20.01.

Adjusing the pH at 8.4, which is used in literature to obtain higher yields in terms of enzymatic activity, in the case of 1Dm15 was not connected to an increase in the release of hydrolytic enzymes (BDL.20.07).

Interestingly in the test BDL.20.02, where the recipe of the media was not supplemented with an additional carbon source, it is possible to appreciate high enzymatic activity (9.3 U/ml) compared to the cell growth which is lower than the additional media (1x10^7 CFU/ml).

A

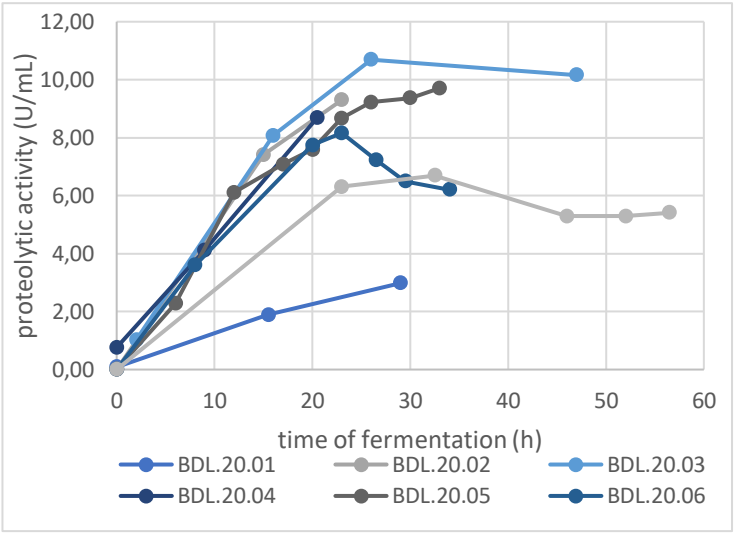

B

test	*Cell growth (CFU/ml)*	*Enzymatic activity (U/ml)*
1	3x10^8	2,98
2	1x10^7	9,3
3	1,2x10^8	10,17
4	2x10^8	8,69
5	2x10^8	9,71
6	2x10^7	6,21
7	1,2x10^7	5,57

Figure 21- A) graph of the different trends in proteolytic activity during the growth, B) final results of cell viability and enzymatic activity.

The supernatants were used for a dehairing test on the pilot scale and the results are showed in Table 22. The BDL.20.01 presented a partial dehairing, which was consistent with the total detected proteolytic activity. The same was observed in the BDL.20.07 where the underhair was still present in the hair bulb. The BDL20.03 and BDL.20.05 presented an over digestion of the epidermidis and a strong attack of the dermis, this resulted in partial degradation of collagen, particularly evident in BDL.20.05 where the hide completely lost its structure. In the BDL.20.04 and BDL.20.06, the complete dehairing needs the help of an oxidative agent to complete the cleaning of the grain and some hair root is still present in the bulb.

The BDL.20.02 presented the best result in terms of dehairing, the hide reported a clean grain and the correct consistency after liming, the epidermidis was completely removed.

TEST	RESULTS
1	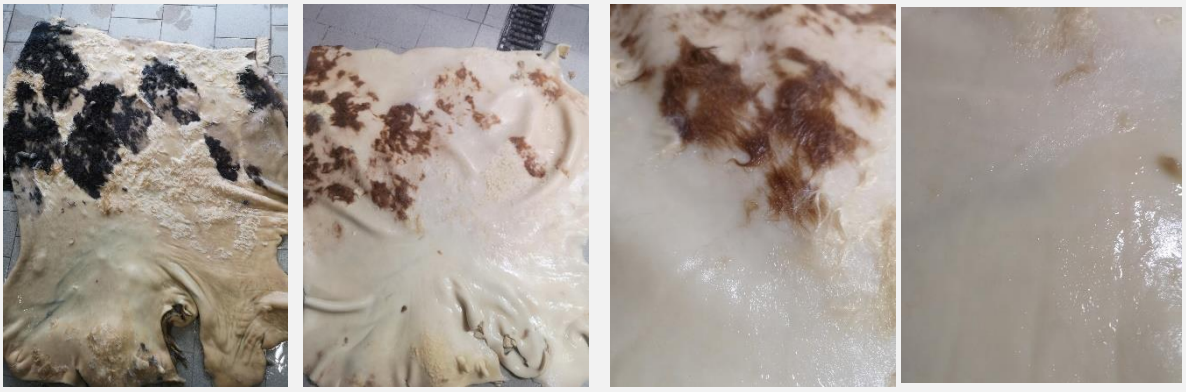
2	
3	

4	
5	
6	
7	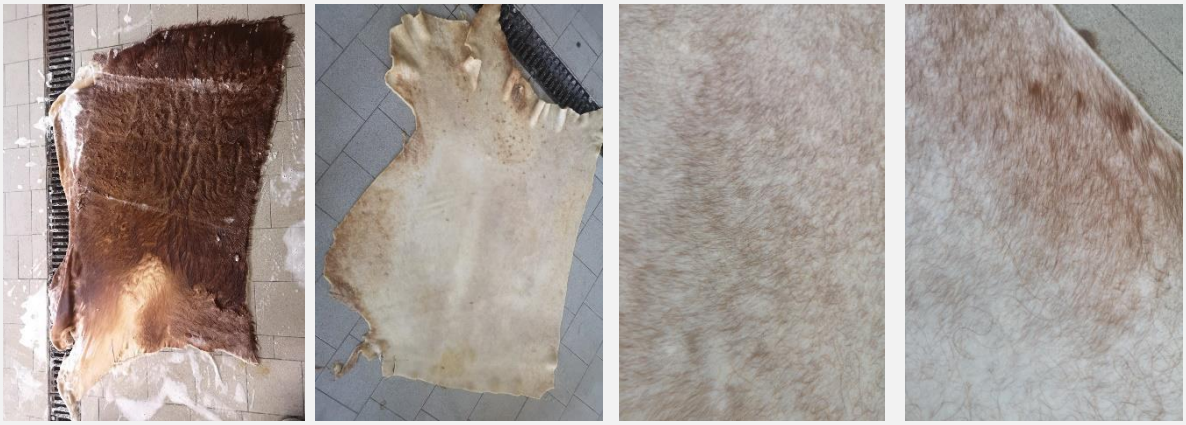

Table 22- results obtained in the dehairing tests of bioreactor surnatant.

The results obtained during the unhairing test as well as the results obtained in the bioreactor growth showed that the protocol of BDL20.02 was the most promising.

PROTEOME ANALYSIS AFTER GROWTH UNDER DIFFERENT CONDITIONS

On the supernatant derived from the tests in the bioreactor was performed a proteomic analysis to look for some consistent differences between them that cleared the mechanism of unhairing.

In Table 23 (Appendix) are reported the proteins detected, which showed high intensities. Interestingly, the top five proteins detected in all the tests are proteases, but in the BDL.20.02, it is possible to appreciate the presence also of an alpha amylase, which resulted to be important in the dehairing process, since the BDL.20.02 is the dehairing test with best results on raw hides.

SCALE UP: GROWTH AND INDUSTRIAL TESTS

All the data analysed during the growth via bioreactor in Biosphere revealed the parameter for the optimal growth, so we were able to perform a scale-up test, to understand how to transport the process from the lab to the industrial reality.

The test was elaborated to perform a growth on a 150-L bioreactor and to treat the supernatant with the different downstream processes to understand the one with a higher yield. The process was reported in Figure 22.

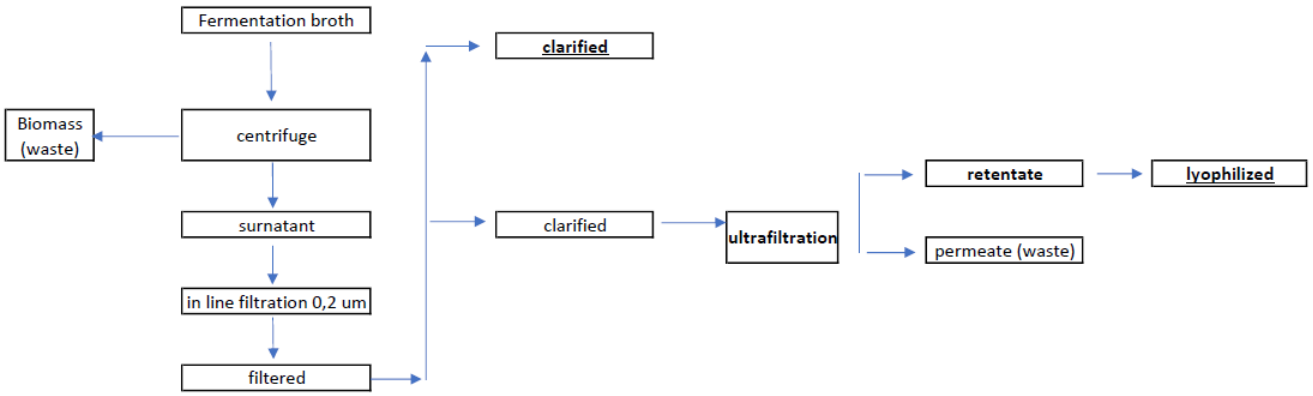

Figure 22- Summary of the process of scale-up

At the end of the culture, the results obtained in terms of cell viability and proteolytic activity were comparable with the one obtained in BDL.20.02 in the 5L bioreactor, as reported in Figure 23 panel A. The slight difference could be due to the fact that fermentation in the 150L test lasts for 24 h instead of 21 h of the BDL20.02, so a partial beginning of cell death and partial degradation of proteases in the media could have begun. In Figure 23 it is possible to appreciate that the trend of proteolytic activity is comparable in both cultures.

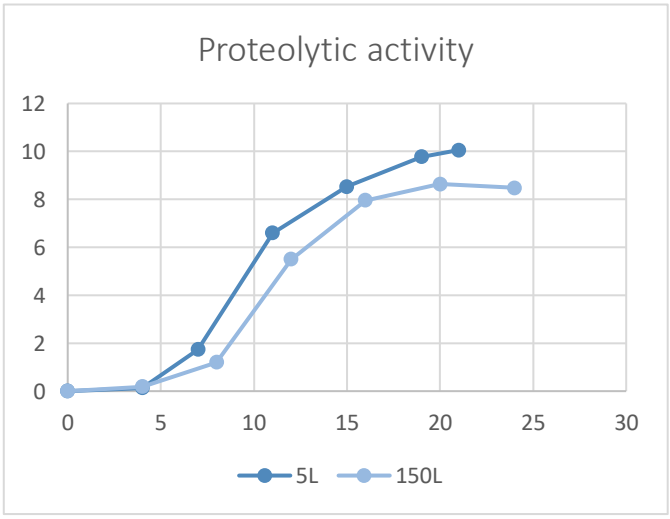

proteolytic final activity	*U/ml*
5L	9,30
150 L	8,38

final cell viability	*CFU/mL*
5L	1,8 x 10^7
150L	6 x 10^7

Figure 23- A) comparison of final data for cell viability and proteolytic activity; B) comparison of trend in proteolytic activity in 5L fermentation respect to 150L

After the growth in the bioreactor, the surnatant was separated from the cellular component of the broth and filtered 0,22 um. Then as reported in figure 22, a part was tested as it is in the unhairing test industrial scale. The remaining part was ultrafiltered, partly tested on an industrial scale and partly tested after the lyophilization.

The results obtained in the industrial test of unhairing were comparable with the obtained previously: clean grain, intact structure of the derma, epidermidis removed, as it is in figure 24.

Figure 24-Dehairing tests of surnatant after filtration.

The interesting observation was that, since the hides that were used were entire, so it was possible to observe the behaviour of the enzymatic treatment on the entire structure of the raw hide, from the belly, that usually is easier to unhair, to the neck zone, which presents a thicker section harder to clean. The obtained result was homogenous all over the hide. We noticed that zones of the hide which were not well conserved, meaning the zones that are already under microorganism attack, were more sensitive to the enzymatic treatment with the risk of ruining the grain. Also, the time of contact between the enzymatic preparation and the hide seemed to be crucial to not cause defects on the final product.

After the ultrafiltration (concentration 1:10) the test was repeated (Figure 25), and the results were confirmed. Also, in this case, it was possible to use entire hides. The advantage is that in the hypothetical industrial process a small amount of ultra-concentrated enzymatic preparation has to be added to the drums. This is considered important for the application in tanneries, where the volume and weight in play are high.

Figure 25-Dehairing tests of surnatant after ultrafiltration.

Once it was ultrafiltered, the remaining surnatant was lyophilized using as a substrate that facilitates the process, maltodextrins. In this case, the volume lyophilized was lower, so it was possible to perform only a pilot-scale unhairing test, which confirmed on the other hand that also in the powder form the surnatant is active and maintains the unhairing ability. The chance to use a powder form product is an important aspect because it is possible to reduce again the amount of product dosed during the process, with the consequences of better storage and simplify the operation of workers. Moreover, the powder form of the product allows extending the shelf life of the preparation

Figure 26-Dehairing tests of surnatant after lyophilization.

It was interesting to observe the behaviour of the proteolytic activity among all the stages of growth and downstream, to understand the percentage of activity that is lost during the manipulation of the supernatant. As it is possible to appreciate in Figure 27, after the filtration of at 550KDa the residual enzymatic activity was 109,4% since the water was added for the filtration process. After the ultrafiltration 10kDa, the residual activity was 91,3%. Moreover, after the lyophilization step was 104% using the maltodextrin at 1%. In all the stages the enzymatic activity was maintained and observed also *in vitro* not only during the unhairing tests. Thanks to the information of Figure 26 it was possible to build up a plan for 1000L scale up step and for industrial production.

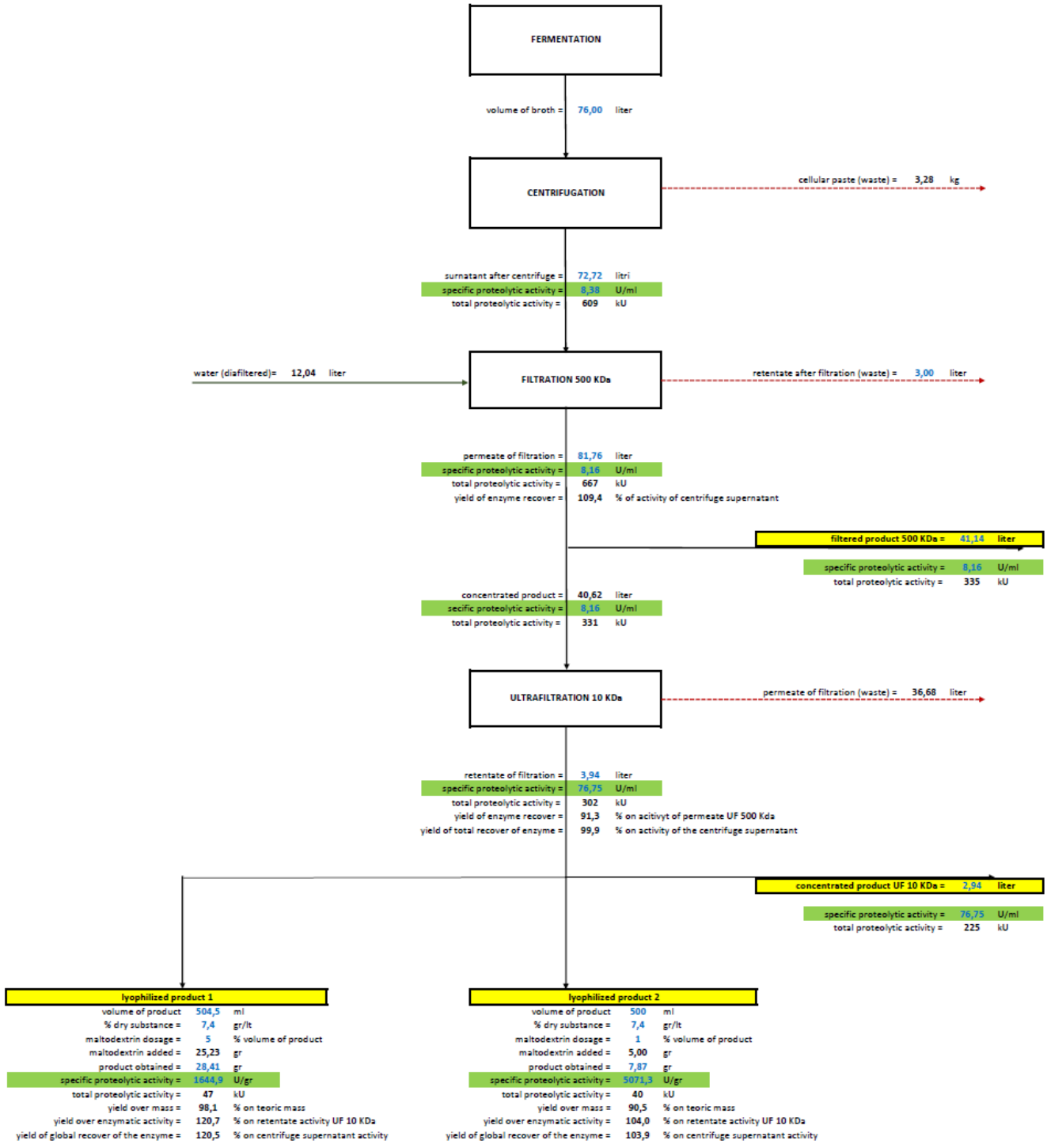

Figure 27- Process of scale up and yields obtained during each step of filtration; after the growth the supernatant is filtered at 500 kDa, a part was tested directly (41.14 L), the rest is ultrafiltered at 10 kDa, partly tested and partly lyophilized using different concentration of maltodextrins as adjuvant. After each step the enzymatic activity is reported and so the yields of recovery.

CONCLUSIONS AND PERSPECTIVES

Bacteria hydrolytic enzymes exhibit a great potential in industrial application being able to conduce reaction in substitution of traditional chemical compounds.

In the case of tanneries, the need of more sustainable solution is an urgent issue. The use of sulphides for the dehairing phase accounts for the main part of the pollution load of the process, causing high costs for the wastewater treatment and consistent problems derived from the smell of H_2S in the nearby of tanneries district. The advantages of enzymatic use will be an improvement in the pollution index in wastewater (COD, BOD, TKN and sulphides), the possibility to recover hair and transform in a new raw material, the health condition of the operators will benefit, and the unhairing process will be conducted at very high quality in less time and saving up water for the treatment.

Enzymatic solutions for the dehairing phase are not yet in commerce, since enzymatic dehairing presented many challenges in terms of costs, uniformity of results and management of the operations. In scientific literature, many works propose the use of enzymes, mainly alkaline proteases or keratinases, able to dehair hides in the laboratory scale. However, many of this presented solution do not take into consideration the parameters of the dehairing phase during tanning process proposing pH or temperature condition for the best enzymatic activity very far from the real setting. In addition, the proposed solution to produce recombinantly the enzymes of interest will bring to costs problems, in fact chemicals compounds used present very low costs and very high efficiency, making them difficult to substitute from an economic point of view. The other disadvantage of using a recombinant enzyme is the absence of enzymatic blends which, according to recent literature, is the key factor for a complete and functional dehairing able to work on the entire section of the hide.

The isolation of a natural strain directly from hides, probably naturally selected for hydrolysing keratin and substrates present on hide skins, have many advantages. The growth process based on poor media and keratin substrates will contain the costs of fermentation; moreover, will consume keratinaceous waste such as chicken feather or cow hair. Advantageously, the enzymatic activity obtained with the

supernatants is not limited to an activity of the protease type but includes several additional enzymatic activities such as glycolytic enzymes and lipolytic enzymes. The presence of heterogenous enzymatic activity facilitate the preservation of the collagen and of the derma and guarantee the complete removal of epidermidis and hair, leaving the grain intact and clean. The scale up of the bacterial growth till an industrial scale and the evidence that the dehairing process can be scale up, is, for our best knowledge, reported for the first time. The working condition of supernatant derived by 1Dm15 are completely coherent with the industrial process, such as pH between 7.0 and 9.0 and temperature over 25°C and below 30°C.

In conclusion, in this study we presented the isolation from cow skins of a bacterial isolate able to secrete an enzymatic blend with dehairing activity. The process of screening among a strains collection leads to the identification of *Bacillus spp*. named 1Dm15, the supernatants of this strain grown in minimal medium can dehair cow skins without damaging the derma and leaving the grain clear. With the application of 1Dm15 supernatant into the dehairing phase the hide structure will not be damaged ensuring the economic value of the hide and finished leather as well as the reduction of pollution index in the wastewater. We also demonstrated the possibility to scale up the process and the maintenance of the dehairing activity even when larger volumes are at stake. The *Bacillus spp.* 1Dm15 show attractive properties suitable to be applied in the efficient and eco-friendly dehairing of leather process industry, as well as in other industrial process which need hydrolyzation of substrate.

APPENDIX

1) Annotation of the XMM secretome of the selected 4 isolates.

PROTEIN ID	ANNOTATION
3AM2_3235	peptidase M6 immune inhibitor A
3AM2_1479	Receptor
3AM2_3497	Belongs to the ompA family
3AM2_286	COG2931, RTX toxins and related Ca2 -binding proteins
3AM2_2713	Catalyses the formation of 6,7-dimethyl-8- ribityllumazine in the biosynthesis of riboflavin

Table 8- Annotation of XMM secretome of 3Am2

PROTEIN ID	ANNOTATION
T2D3_2919	2-oxoglutarate translocator
T2D3_1434	Alpha-2-macroglobulin family
T2D3_4570	arginyl-trna synthetase
T2D3_2474	Aromatic hydrocarbon degradation protein
T2D3_3687	Belongs to the glycosyl hydrolase 28 family
T2D3_2321	Belongs to the ompA family
T2D3_2389	Belongs to the ompA family
T2D3_2388	Belongs to the ompA family
T2D3_3905	Belongs to the peptidase S1B family
T2D3_259	Carboxypeptidase regulatory-like domain
T2D3_1112	Cellulase (glycosyl hydrolase family 5)
T2D3_280	Chromophore lyase
T2D3_3579	Collagen-binding protein
T2D3_3447	Conserved repeat domain
T2D3_471	C-terminal domain of CHU protein family
T2D3_2576	C-terminal domain of CHU protein family
T2D3_281	C-terminal domain of CHU protein family
T2D3_4579	Domain of unknown function (DUF4136)
T2D3_3067	Endonuclease I
T2D3_2263	Family of unknown function (DUF5458)
T2D3_2369	Fibronectin type 3 domain
T2D3_1589	Fibronectin type 3 domain
T2D3_2233	Fibronectin type 3 domain
T2D3_1034	Fibronectin type 3 domain
T2D3_1588	Fibronectin type III domain
T2D3_2995	Flagellar motor protein MotB
T2D3_2387	Flagellar motor protein MotB
T2D3_3165	Gliding motility protein

T2D3_1569	Gliding motility protein
T2D3_1568	gliding motility protein
T2D3_2636	Gliding motility protein
T2D3_1567	gliding motility protein
T2D3_3877	Hep Hag repeat protein
T2D3_2637	IgGFc binding protein
T2D3_4233	IgGFc binding protein
T2D3_444	Isoleucyl-tRNA synthetase
T2D3_276	Legume-like lectin family
T2D3_277	Legume-like lectin family
T2D3_3012	LemA family
T2D3_2611	Leucine-rich repeat (LRR) protein
T2D3_1276	Leucyl aminopeptidase
T2D3_2917	Linear amide C-N hydrolases, choloylglycine hydrolase family
T2D3_296	Lipid A 3-O-deacylase (PagL)
T2D3_714	Lipocalin-like domain
T2D3_2190	Lipocalin-like domain
T2D3_2232	Metallo-peptidase family M12B Reprolysin-like
T2D3_1548	Metalloprotease
T2D3_520	OmpW family
T2D3_2578	Outer membrane efflux protein
T2D3_1240	Outer membrane protein beta-barrel domain
T2D3_166	Outer membrane protein beta-barrel domain
T2D3_517	Outer membrane protein beta-barrel domain
T2D3_732	Outer membrane protein SusF_SusE
T2D3_2815	Outer membrane receptor protein
T2D3_4545	Part of the outer membrane protein assembly complex, which is involved in assembly and insertion of beta-barrel proteins into the outer membrane
T2D3_1346	Penicillin-binding protein
T2D3_869	Peptidase C1-like family
T2D3_2155	Peptidase family C25
T2D3_3958	Peptidase M1
T2D3_4622	Peptidase M42
T2D3_4036	Peptidoglycan-binding protein LysM
T2D3_1631	Phage major capsid protein E
T2D3_2918	Phosphate-selective porin O and P
T2D3_4546	PKD domain
T2D3_3326	PorT protein
T2D3_2609	Pregnancy-associated plasma protein-A
T2D3_2448	Protein of unknown function (DUF3078)
T2D3_2921	SdhA B are the catalytic subcomplex and can exhibit succinate dehydrogenase activity in the absence of SdhC D which are the membrane components and form cytochrome b556
T2D3_3697	Secretory lipase
T2D3_2583	Starch-binding associating with outer membrane
T2D3_3756	Starch-binding associating with outer membrane
T2D3_1591	Subtilase family
T2D3_3938	Subtilase family

T2D3_1759	Superoxide dismutase
T2D3_2612	Tail Collar
T2D3_4402	TIGRFAM Por secretion system C-terminal sorting domain
T2D3_2582	TonB dependent receptor
T2D3_3201	TonB dependent receptor
T2D3_734	TonB dependent receptor
T2D3_4152	TonB dependent receptor
T2D3_958	TonB-dependent receptor
T2D3_3620	TonB-dependent receptor
T2D3_604	TonB-dependent receptor
T2D3_92	TonB-dependent receptor
T2D3_2015	TonB-dependent Receptor Plug Domain
T2D3_3757	TonB-dependent Receptor Plug Domain
T2D3_3020	Type IX secretion system membrane protein PorP/SprF
T2D3_2264	Type VI secretion system, VipA, VC_A0107 or Hcp2
T2D3_1079	Vgr family
T2D3_2616	Von Willebrand factor A
T2D3_4023	no annotations
T2D3_518	no annotations
T2D3_4461	no annotations
T2D3_2909	no annotations
T2D3_1498	no annotations
T2D3_671	no annotations
T2D3_4001	no annotations
T2D3_1695	no annotations
T2D3_159	no annotations
T2D3_2055	no annotations
T2D3_4552	no annotations
T2D3_2004	no annotations
T2D3_2742	no annotations
T2D3_2792	no annotations
T2D3_4154	no annotations

Table 9- Annotation of XMM secretome of T2D3

PROTEIN ID	ANNOTATION
1DM8_340	beta-galactosidase
1DM8_197	3-hydroxyacyl-CoA dehydrogenase
1DM8_3899	A type II topoisomerase that negatively supercoils closed circular double-stranded (ds) DNA in an ATP-dependent manner to modulate DNA topology and maintain chromosomes in an underwound state. Negative supercoiling favors strand separation, and DNA replication, transcription, recombination and repair, all of which involve strand separation. Also able to catalyze the interconversion of other topological isomers of dsDNA rings, including catenanes and knotted rings. Type II topoisomerases break and join 2 DNA strands simultaneously in an ATP-dependent manner
1DM8_2048	ABC transporter substrate-binding protein
1DM8_1438	Acetylornithine deacetylase

1DM8_3701	acetyltransferases and hydrolases with the alpha beta hydrolase fold
1DM8_1688	Acts on the D-isomers of alanine, leucine, aspartate, glutamate, aminobutyrate, norvaline and asparagine. The enzyme transfers an amino group from a substrate D-amino acid to the pyridoxal phosphate cofactor to form pyridoxamine and an alpha- keto acid in the first half-reaction
1DM8_195,1DM8_3791,1DM8_669	acyl-CoA dehydrogenase
1DM8_3333	Alpha beta hydrolase
1DM8_2420	alpha-L-arabinofuranosidase activity
1DM8_2442	Alpha-L-arabinofuranosidase C-terminus
1DM8_696,1DM8_695	amine dehydrogenase activity
1DM8_1182	Belongs to the bacterial solute-binding protein 3 family
1DM8_2222	Belongs to the Dps family
1DM8_3591	Belongs to the glycosyl hydrolase 26 family
1DM8_3603	Belongs to the glycosyl hydrolase 3 family
1DM8_2606	Belongs to the glycosyl hydrolase 32 family
1DM8_3877	Belongs to the glycosyl hydrolase 43 family
1DM8_435	Belongs to the metallo-dependent hydrolases superfamily. NagA family
1DM8_3652	Belongs to the peptidase S1B family
1DM8_2751	Belongs to the peptidase S8 family
1DM8_3604	Belongs to the UPF0214 family
1DM8_3746	Catalyzes the ATP-dependent amidation of deamido-NAD to form NAD. Uses ammonia as a nitrogen source
1DM8_1321	Catalyzes the Claisen rearrangement of chorismate to prephenate. Probably involved in the aromatic amino acid biosynthesis
1DM8_2412	Catalyzes the conversion of L-arabinose to L-ribulose
1DM8_3978	Catalyzes the interconversion of ornithine to glutamate semialdehyde
1DM8_1377	Catalyzes the isomerization of 5-dehydro-4-deoxy-D- glucuronate to 3-deoxy-D-glycero-2,5-hexodiulosonate
1DM8_276	Catalyzes the reductive cleavage of azo bond in aromatic azo compounds to the corresponding amines. Requires NADH, but not NADPH, as an electron donor for its activity
1DM8_638	Catalyzes the reversible interconversion of serine and glycine with tetrahydrofolate (THF) serving as the one-carbon carrier. This reaction serves as the major source of one-carbon groups required for the biosynthesis of purines, thymidylate, methionine, and other important biomolecules. Also exhibits THF- independent aldolase activity toward beta-hydroxyamino acids, producing glycine and aldehydes, via a retro-aldol mechanism
1DM8_2296	COG0491 Zn-dependent hydrolases, including glyoxylases
1DM8_2227	COG0715 ABC-type nitrate sulfonate bicarbonate transport systems, periplasmic components
1DM8_2051	COG0791 Cell wall-associated hydrolases (invasion-associated proteins)
1DM8_1335	COG1290 Cytochrome b subunit of the bc complex
1DM8_2300	COG1363 Cellulase M and related proteins
1DM8_3050	COG1762 Phosphotransferase system mannitol fructose-specific IIA domain (Ntr-type)
1DM8_2434	COG1796 DNA polymerase IV (family X)
1DM8_3045	COG2309 Leucyl aminopeptidase (aminopeptidase T)
1DM8_265	Component of the sulfite reductase complex that catalyzes the 6-electron reduction of sulfite to sulfide. This is one of several activities required for the biosynthesis of L- cysteine from sulfate. The flavoprotein component catalyzes the electron flow from NADPH - FAD - FMN to the hemoprotein component

1DM8_2579	cystathionine
1DM8_2044	D-aminopeptidase
1DM8_996	Deoxyribonuclease NucA/NucB
1DM8_747	Essential for the localization of CwlJ in the spore coat and for spore germination triggered by calcium and dipicolinic acid (DPA). Its assembly into the spore coat is dependent on the coat morphogenetic proteins CotE and SpoIVA
1DM8_1771	Excalibur calcium-binding domain
1DM8_634	F(1)F(0) ATP synthase produces ATP from ADP in the presence of a proton or sodium gradient. F-type ATPases consist of two structural domains, F(1) containing the extramembraneous catalytic core and F(0) containing the membrane proton channel, linked together by a central stalk and a peripheral stalk. During catalysis, ATP synthesis in the catalytic domain of F(1) is coupled via a rotary mechanism of the central stalk subunits to proton translocation
1DM8_1142	first, biotin carboxylase catalyzes the carboxylation of the carrier protein and then the transcarboxylase transfers the carboxyl group to form malonyl-CoA
1DM8_4209	Glycoside Hydrolase Family
1DM8_3789	Glycosyl hydrolase-like 10
1DM8_790	glyoxalase
1DM8_2422	Glyoxalase-like domain
1DM8_1311	Histone-like DNA-binding protein which is capable of wrapping DNA to stabilize it, and thus to prevent its denaturation under extreme environmental conditions
1DM8_1819	hydrolases or acyltransferases (alpha beta hydrolase superfamily)
1DM8_2752,1DM8_3942	Metallo-beta-lactamase superfamily
1DM8_2735	n-acetylmuramoyl-L-alanine amidase
1DM8_116	NADH dehydrogenase
1DM8_381	Patatin-like phospholipase
1DM8_3372	Pectate lyase superfamily protein
1DM8_1358	penicillin-binding protein
1DM8_129	peptidase
1DM8_3984	Permuted papain-like amidase enzyme, YaeF/YiiX, C92 family
1DM8_3613	protein conserved in bacteria
1DM8_3602	protein conserved in bacteria
1DM8_3582	Protein of unknown function (DUF1541)
1DM8_3033	Removes the formyl group from the N-terminal Met of newly synthesized proteins. Requires at least a dipeptide for an efficient rate of reaction. N-terminal L-methionine is a prerequisite for activity but the enzyme has broad specificity at other positions
1DM8_1313	Required for transcription attenuation control in the Trp operon. This trans-acting factor seems to recognize a 10 bases nucleotide sequence in the Trp leader transcript causing transcription termination. Binds the leader RNA only in presence of L-tryptophan
1DM8_736	Spore Coat
1DM8_2777	Spore coat protein
1DM8_1911	Spore coat protein Z
1DM8_1430	no annotation

Table 10- Annotation of XMM secretome of 1Dm8

PROTEIN ID	ANNOTATION
1DM15_1143	4-aminobutyrate aminotransferase
1DM15_1279	esterase /S33 unassigned peptidase
1DM15_1332	glycerophosphodiester phosphodiesterase
1DM15_1370	esterase / ybbE
1DM15_1455	cytochrome B
1DM15_1883	beta-galactosidase
1DM15_1884	Arabinogalactan endo-1,4-beta-galactosidase
1DM15_1939	azoreductase
1DM15_204	cystathionine beta-lyase
1DM15_2147	DppE
1DM15_2151	D-aminopeptidase / M55 unassigned peptidase
1DM15_2410	Excalibur calcium-binding domain
1DM15_2492	D-alanine aminotransferase
1DM15_2711	diacetylchitobiose-6-phosphate hydrolase
1DM15_2834	conserved hypothetical protein / S9 non-peptidase homologues
1DM15_3361	ATP synthase F0 subunit C
1DM15_3402	exported mannan endo-1,4-beta-mannosidase
1DM15_3528	D-alanyl-D-alanine carboxypeptidase/D-alanyl-D-alanine-endopeptidase
1DM15_355	glyoxalase family protein
1DM15_3646	acyl-CoA dehydrogenase
1DM15_4208	cell-division protein and general stress protein (class III heat-shock) / FtsH-2 peptidase
1DM15_4217	Dihydroneopterin aldolase
1DM15_744	cytochrome Cbb3
1DM15_746	menaquinol:cytochrome c oxidoreductase iron-sulfur subunit
1DM15_1168	hypothetical protein
1DM15_122	hypothetical protein
1DM15_1320	hypothetical protein
1DM15_1371	hypothetical protein
1DM15_1372	hypothetical protein
1DM15_1683	hypothetical protein
1DM15_2191	hypothetical protein
1DM15_2833	hypothetical protein / S9 non-peptidase homologue
1DM15_3287	hypothetical protein
1DM15_3411	hypothetical protein
1DM15_343	hypothetical protein
1DM15_3642	hypothetical protein
1DM15_3776	hypothetical protein
1DM15_3979	hypothetical protein
1DM15_1023	phosphate ABC transporter binding lipoprotein
1DM15_1232	NAD synthetase
1DM15_1399	PTS fructose transporter subunit IIA / S9 non-peptidase homologue
1DM15_1684	serine protease /AprX peptidase
1DM15_1694	RNA-binding protein Hfq
1DM15_1701	N-acetylmuramoyl-L-alanine amidase

1DM15_1795	N-acetylglucosamine-6-phosphate deacetylase / M38 non-peptidase homologue
1DM15_2122	serine protease / IspA peptidase
1DM15_2144	peptidase / NLP-P60 Nostoc-like putative peptidase
1DM15_2599	penicillin acylase
1DM15_2617	urocanate hydratase
1DM15_2781	spore coat and germination protein GerQ
1DM15_2792	spore coat protein
1DM15_3365	Serine hydroxymethyltransferase
1DM15_3724	putative xylanase/chitin deacetylase
1DM15_3840	ornithine--oxo-acid aminotransferase
1DM15_3846	YycO
1DM15_4229	YusJ
1DM15_469	peptidase M28 / glutamyl aminopeptidase
1DM15_498	peptide ABC transporter substrate-binding protein
1DM15_61	sporulation protein
1DM15_698	peptidase M32
1DM15_722	penicillin-binding protein
1DM15_985	spore coat protein N

Table 11- Annotation of XMM secretome of 1Dm15

2) Protein selected by intensity in the 4 selected isolates.

Protein IDs	*% intensity 1Dm8-FMM*		*Protein IDs2*	*% Intensity 1Dm8-NB*		*Protein IDs4*	*% Intensity 1Dm8-WMM*	
Bio05_2073	13,7	major intracellular serine protease	Bio05_2954	18,2	bacillopeptidase F precursor	Bio05_1877	13,2	oligopeptide ABC transporter
Bio05_1753	8,9	subtilisin E	Bio05_2630	10,1	hypothetical protein	Bio05_1753	11,2	subtilisin E
Bio05_3016	8,8	bacillolysin, extrac metalloprotease	Bio05_445	10,0	flagellin protein flaA	Bio05_2751	5,7	serine protease AprX
Bio05_1877	7,3	oligopeptide ABC transporter	Bio05_2622	5,5	chitosane precursor	Bio05_2954	5,6	bacillopeptidase F precursor
Bio05_2751	5,0	serin protease AprX	Bio05_3016	5,4	bacillolysin, extrac metalloprotease	Bio05_2073	5,4	intra serine protease
Bio05_862	4,1	endo beta glucanase	Bio05_1753	5,1	subtilisin E	Bio05_761	4,9	minor extrac protease VPR
Bio05_2735	3,4	hypothetical protein	Bio05_3737	3,2	alpha-amylase	Bio05_3652	3,9	glutamyl endopeptidase precursor
Bio05_3027	3,3	dihydrolipoamide dehydrogenase ()	Bio05_938	2,6	cell surface protein	Bio05_862	3,7	endo beta glucanase
Bio05_2954	3,2	bacillopeptidase F precursor	Bio05_3861	2,4	hypothetical protein	Bio05_3016	3,2	bacillolysin, extrac metalloprotease
Bio05_1073	3,2	superoxide dismutase	Bio05_3027	2,0	dihydrolipoamide dehydrogenase (pyruvate)	Bio05_1073	3,0	superoxide dismutase
Bio05_1601	2,9	catalase KatE	Bio05_862	1,5	endo beta glucanase	Bio05_3027	2,7	dihydrolipoamide dehydrogenase (pyruvate)
Bio05_761	2,6	minor extrac protease VPR	Bio05_1073	1,4	superoxide dismutase	Bio05_1601	2,3	catalse kat e
Bio05_10	2,6	hypothetical protein	Bio05_1585	1,4	gamma-gòutamyltranspeptidase	Bio05_2048	2,1	dipeptide ABC transporte
Bio05_1430	1,6	outermost layer of spore	Bio05_801	1,3	arginyl aminopeptidase	Bio05_801	1,9	arginyl aminopeptidase
Bio05_1115	1,6	biofilm matrix component	Bio05_1562	1,3	expasin yoaJ	Bio05_2735	1,6	sporulation amidase
Bio05_3258	1,6	phosphodiesterase	Bio05_2618	1,2	membrane protein related to metallopeptidase	Bio05_1430	1,6	outer membrane of spore
Bio05_3737	1,6	alpha-amylase	Bio05_2444	1,2	thioredoxin	Bio05_3737	1,4	alpha-amylase
Bio05_3652	1,5	glutamyl endopeptidase	Bio05_3805	1,1	xylanase	Bio05_3258	1,3	phosphodiesterase
Bio05_163	1,0	extrac ribonuclease	Bio05_2617	1,1	membrane protein related to metallopeptidase	Bio05_1190	1,1	peptidase yqjE
			Bio05_429	1,0	type II effector, pectate lyase	Bio05_1805	1,0	protease WprA

Table 12- Annotated protein selected by intensity of 1Dm8

Protein IDs	*% Intensity 1Dm15-FMM*		*Protein IDs*	*% Intensity 1Dm15-NB*		*Protein IDs*	*% Intensity 1Dm15-WMM*	
Bio07_1434	13,8	bacilluslysin, neutral metalloprotease	Bio07_3713	9,4	hypothetcal protein	Bio07_2426	17,1	subtilisin E
Bio07_2426	9,9	subtilisin E	Bio07_2426	9,4	subtilisin E	Bio07_2122	10,5	major intrac serine protease precursor
Bio07_2122	7,8	major intr serin protease precursor	Bio07_148	8,3	chitosanase precursor	Bio07_1434	9,5	bacillolysin extra metalloprotease
Bio07_1498	5,2	bacillopeptidase F rpecursor	Bio07_2261	5,5	hypothetical protein	Bio07_1321	6,9	glutamyl endopeptidase precursor
Bio07_985	4,6	stationary phase secreted protein	Bio07_3347	4,1	d amino acid dehydrogenase large subunit	Bio07_2765	6,9	minor extrac protease Vpr
Bio07_2765	4,4	minor extra protease VPr	Bio07_1026	3,8	superoxide dismutase	Bio07_1498	3,9	bacillopeptidase F precursor
Bio07_1026	3,4	superoxide dismutase	Bio07_1423	3,6	dihydrolipoamide dehydrogenase of pyruvate	Bio07_2583	2,7	catalase katE
Bio07_1423	3,0	dihydrolipoamide dehydrogenase ()	Bio07_2723	3,4	arginyl aminopeptidase	Bio07_1026	2,5	superoxide dismutase
Bio07_3226	2,7	hypotetical protein	Bio07_333	3,4	thioredoxin	Bio07_2658	2,5	endo beta glucanase
Bio07_2583	2,5	vatalase KatE	Bio07_1434	2,9	bacillolysin extra metalloprotease	Bio07_2723	2,5	arginyl aminopeptidase
Bio07_1763	2,3	flagellin protein	Bio07_3560	2,7	expasin YoaJ	Bio07_3535	2,5	gamma-glutamy transpeptidase
Bio07_2317	2,0	oligopeptide ABC trasporter	Bio07_4054	2,3	cell surface protein	Bio07_2147	2,3	dipeptide abc trnsporter
Bio07_3878	2,0	phosphodiesterasi	Bio07_1674	2,2	hypothetical protein	Bio07_1684	2,2	serin protease AprX
Bio07_1242	1,7	alpha-amylase	Bio07_3535	1,9	gamma-glutamyltranspeptidase	Bio07_1423	1,9	dihydrolipoamide dehydrogenase of pyruvate
Bio07_908	1,5	peptidase YqjE	Bio07_3072	1,7	extrac ribonuclease	Bio07_916	1,6	arginine- binding extracellular protein
Bio07_1684	1,3	serine protease AprX	Bio07_1498	1,5	bacillopeptidase F precursor	Bio07_1242	1,5	alpha-amylase
Bio07_2306	1,3	oligoendopeptidase F	Bio07_4108	1,3	lsu ribosomal protein	Bio07_3878	1,5	hypothetical protein
Bio07_3010	1,1	homoserine kinase	Bio07_1242	1,2	alpha-amylase	Bio07_3072	1,2	extrac ribonuclease
Bio07_3072	1,0	extrac ribonuclease	Bio07_653	1,2	3-phytase	Bio07_333	1,0	thioredoxin
Bio07_2658	1,0	endo beta glucanase	Bio07_400	1,1	malate dehydrogenase			
Bio07_3304	1,0	collagen adhesion protein	Bio07_1343	1,1	hypothetical protein			
Bio07_1321	1,0	glutamyl endopeptidase	Bio07_908	1,1	peptidase YqjE			

Table 12- Annotated protein selected by intensity of 1Dm15

Protein IDs	*% Intensity 3mA2-FMM*		*Protein IDs*	*% Intensity 3mA2-NB*		*Protein IDs*	*% Intensity 3mA2-WMM*	
Bio01_1880	21,4	flagellin protein flaA	Bio01_2674	9,9	hypothetical protein	Bio01_1880	43,8	flagellin protein
Bio01_1388	8,2	pullulanase	Bio01_1880	9,3	flagellin protein flaA	Bio01_4385	12,3	t1ss segreted agglutinin rtx
Bio01_1849	7,6	maltodextrin abc trasporter	Bio01_34	5,5	lipoprotein	Bio01_1479	7,6	tonB receptor
Bio01_1269	6,6	vibriolysin extra zinc protease	Bio01_4022	5,0	hemolysin	Bio01_3235	5,6	metalloprotease zinc binding
Bio01_971	3,6	isocitrate lyase	Bio01_1882	4,4	flagellar cap protein FliD	Bio01_1269	4,9	vibriolysin extrac zinc protease
Bio01_111	3,1	maltoporin	Bio01_3499	4,2	phospholipase lecithinase hemolysin	Bio01_286	4,5	t1ss segreted agglutinin rtx
Bio01_1879	2,8	flasellin protein flA	Bio01_3765	3,6	beta- lytic metallopeptidase	Bio01_3772	4,2	lipoprotein
Bio01_791	2,6	galactose methyl abc trsporte	Bio01_1269	3,5	vibrilysin extrac xinc protease	Bio01_459	3,6	extrac deoxyribonylease
Bio01_1479	2,3	ton B depedent receptor	Bio01_2924	3,3	citolysin hemolysin	Bio01_111	3,3	maltoporin
Bio01_2370	1,9	dihydrolipoamide dehydrogenase of pyrivate	Bio01_1849	3,1	maltodextrin Abc trnsporte	Bio01_1002	2,9	outer membrane porin
Bio01_949	1,9	flagellar hook protein	Bio01_271	2,7	extrac protease precursor	Bio01_1879	2,8	flagellin protein
Bio01_1084	1,4	phosphoenolpyruvate carboxykinase	Bio01_225	2,4	leucin aminopeptidase	Bio01_2250	1,2	lipase
Bio01_1002	1,4	outermembrane porin ompC	Bio01_2563	2,2	chitinase			
Bio01_1332	1,3	nad dep glyceraldeide phosphate dehydrogenase	Bio01_3751	2,0	trap transporte solute receptor			
Bio01_3772	1,3	lipoprotein	Bio01_1253	1,9	alpha-amylase			
Bio01_3225	1,2	lipoprotein YgdR	Bio01_4385	1,9	T1ss secreted agglutinin			
Bio01_2185	1,2	glycosidase	Bio01_1134	1,8	collagenase			
Bio01_564	1,0	hypothetical protein	Bio01_836	1,5	putrescin trnsporte			
Bio01_4385	1,0	T1aa secreted agglutin RTXhyp	Bio01_955	1,3	flagellar hook protein			
			Bio01_2496	1,2	hypothetical protein			
			Bio01_3772	1,2	g111135 protein			
			Bio01_2562	1,2	lipoprotein			

Table 13 Annotated protein selected by intensity of 3Am2

Potein IDs	*% Intensity T2D3-FMM*		*Protein IDs*	*% Intensity T2D3-NB*		*Protein IDs*	*% Intensity T2D3-WMM*	
Bio10_3145	9,2	peptidase S8 secreted	Bio10_749	31,4	LPMO superfamily	Bio10_3145	11,7	peptidase S8 secreted
Bio10_1249;Bio10_1876	6,2	hypothetical protein	Bio10_3145	16,2	peptidase S8 secreted	Bio10_3291	7,8	hypothetical protein
Bio10_4627	5,2	susD/ Rag A membrane lipoprotein	Bio10_2642	9,7	hypothetical / MACPF domain	Bio10_3151	5,2	T9SS secreted protein
Bio10_1677	5,0	hypothetical protein	Bio10_3291	5,3	hypothetical protein	Bio10_1698	5,0	bacteriocin / hypothetical protein
Bio10_3151	3,5	T9SS secreted protein	Bio10_3151	4,6	T9SS secreted protein	Bio10_4377	4,7	susD /ragA nutrient uptake
Bio10_3291	3,4	hypothetical protein	Bio10_4436	2,3	hypothetical protein	Bio10_749	4,0	LPMO superfamily
Bio10_1696	3,3	bacteriocin / hypothetical protein	Bio10_2823	2,2	metalloprotease Zn	Bio10_4627	3,9	susD/ Rag A membrane lipoprotein
Bio10_2524	3,2	hypothetical / bacteriocin	Bio10_2402	1,8	Zn Mc metalloprotease	Bio10_1249; Bio10_1876	3,5	hypothetical protein
Bio10_1698	2,9	bacteriocin / hypothetical protein	Bio10_2376	1,6	secreted protein T9SS/ domain for adhesion	Bio10_1677	3,2	hypothetical protein
Bio10_4378	2,6	susC ragA ligand gate channel fe	Bio10_3347	1,6	hypothetical protein	Bio10_4378	2,8	susC ragA ligand gate channel fe
Bio10_2402	2,4	Zn Mc metalloprotease	Bio10_1925	1,5	hypothetical protein	Bio10_2909	2,6	hypotehtical
Bio10_4436	2,4	hypothetical protein	Bio10_1828	1,2	hypothetical protein	Bio10_4436	2,6	hypothetical protein
Bio10_4626	2,4	susD/ Rag A membrane lipoprotein	Bio10_4563	1,1	peptidase S8 secreted	Bio10_2402	2,5	Zn Mc metalloprotease
Bio10_4377	2,4	susD /ragA nutrient uptake	Bio10_1696	1,1	bacteriocin / hypothetical protein	Bio10_2004	2,2	hypothetical / bacteriocin
Bio10_749	2,3	LPMO superfamily	Bio10_3934	1,0	hypothetical protein	Bio10_4546	2,0	hypothetical PKD domain
Bio10_1807	2,2	ompA domain protein	Bio10_4377	1,0	cell surface glycan lipoprotein	Bio10_2420	1,9	hypothetical protein
Bio10_3697	2,1	hypothetical protein				Bio10_2524	1,8	hypothetical / bacteriocin
Bio10_1279;Bio10_1278	1,9	aminopeptidase				Bio10_2422	1,5	hypothetical protein
Bio10_3934	1,7	hypothetical protein				Bio10_4626	1,5	susD/ Rag A membrane lipoprotein
Bio10_2637	1,5	gliding motility associated				Bio10_3697	1,3	hypothetical protein
Bio10_2909	1,5	hypothetical protein				Bio10_690	1,2	hypothetical protein
Bio10_4546	1,5	hypothetical PKD domain				Bio10_1807	1,2	ompA domain protein
Bio10_2422	1,4	hypothetical protein				Bio10_3938	1,2	peptidase S8 secreted
Bio10_2233	1,3	FN3 domain T9SS				Bio10_2232	1,1	ZnMC metalloprotease FN3 domain
Bio10_2420	1,0	hypothetical protein				Bio10_1696	1,1	bacteriocin / hypothetical protein
						Bio10_2637	1,0	gliding motility associated

Table 15- Annotated protein selected by intensity of T2D3

3)Summary of protein detected in the different growth

Fasta headers	*Protein identification*	*% INT C1*	*% INT C2*	*% INT C3*	*% INT C4*	*% INT C5*	*% INT C6*	*% INT C7*
Bio07_2426	Subtilisin E	1,85	18,70	13,34	22,27	13,44	21,95	16,26
Bio07_1434	Bacillolysin, neutral metalloprotease	0,76	20,65	9,45	16,20	17,44	0,22	0,00
Bio07_2583	Catalase Kat E	14,16	2,27	9,54	0,22	0,14	14,23	7,94
Bio07_1242	Alpha-amylase	0,04	4,64	4,18	0,98	6,53	4,51	8,46
Bio07_561	manganase ABC transporter	1,70	3,15	4,30	0,52	0,23	3,50	10,05
Bio07_1498	Bacillopeptidase F precursor	0,24	2,03	2,93	1,08	5,75	6,02	1,66
Bio07_2317	Oligopeptide ABC transporter	3,81	4,04	1,14	0,18	0,47	0,35	0,37
Bio07_3907	Pectate lyase precursor	0,20	1,67	3,09	15,97	1,93	3,56	0,63
Bio07_2658	Endo beta 1,3-1,4 glucanase	0,23	3,32	1,86	2,27	1,85	2,90	4,02
Bio07_2765	minor extracellualr protease	0,02	5,83	2,31	4,34	0,80	4,26	0,05
Bio07_1026	Superoxide dismutase	3,15	0,50	2,99	0,02	0,18	0,81	3,80
Bio07_3878	2'.3'-cyclic-nucleotide 2'-phosphodiesterase	0,04	2,94	0,76	0,13	0,46	1,36	4,41
Bio07_1223	delta-1-pyrroline-5-carboxylate dehydrogenase	0,83	0,82	3,63	0,12	1,34	0,03	0,00
Bio07_2306	Oligoendopeptidase F	1,77	0,69	2,73	0,00	0,00	1,88	2,22
Bio07_1763	Flagellin peotein	7,41	0,87	1,06	0,60	2,43	0,45	0,00
Bio07_1674	hypothetical protein	0,02	0,28	0,18	0,17	5,49	0,15	0,46
Bio07_985		0,01	0,21	0,48	0,02	0,97	5,37	0,02
Bio07_3713	hypothetical protein	1,27	0,09	0,03	0,18	5,15	0,04	0,62
Bio07_1343	hypothetical protein	0,06	1,55	1,20	1,98	1,88	0,69	1,02
Bio07_3072	extracellular ribonuclease	0,01	0,90	1,35	3,55	3,10	0,01	0,00
Bio07_3010	Homoserine kinase	0,14	0,98	3,31	0,02	0,00	0,33	0,22
Bio07_2246	uncharacterized protein	0,00	0,23	1,07	1,19	1,88	0,61	0,57
Bio07_2653		0,00	2,62	0,35	1,05	0,39	0,00	2,02
Bio07_2793	hypothetical protein	0,40	0,85	0,95	0,92	0,66	0,66	1,27
Bio07_1374	Fe-bacillibactin uptake system	1,05	0,84	0,27	0,22	0,24	0,80	2,06
Bio07_1902	2,3-bisphophoglycerate-indipendent phosphoglycerate mutase	2,15	0,42	0,89	0,00	0,07	1,32	0,81
Bio07_2541	Putative endonuclease	0,01	1,33	0,90	1,16	1,10	0,21	0,40
Bio07_2261	Hypothetical protein	0,01	0,16	0,13	6,64	2,31	0,03	0,05
Bio07_1701		0,00	0,01	1,38	0,00	0,00	1,88	1,13
Bio07_4054	Cell surface protein	0,17	0,44	0,44	2,21	2,14	0,07	0,10
Bio07_3659	Glucuronoarabinoxylan endo-1,4-xylanase	0,11	0,34	0,80	0,86	1,72	0,45	0,25
Bio07_1954	Glyoxal reductase/ methylglyoxal reductase	0,95	0,54	1,41	0,04	0,20	0,54	0,07
Bio07_2675	tripeptide aminopeptidase	0,35	0,44	1,11	0,00	0,16	1,44	0,41
Bio07_2323	Oligopeptide ABC transporter	0,14	0,13	0,01	0,00	0,19	0,00	1,65
Bio07_1423	dihydrolipoamide dehydrogenase of pyruvate dehydrogenase	1,81	0,12	0,54	0,00	0,00	1,76	0,28
Bio07_3347	D-amino acid dehydrogenase large subunit	0,00	0,00	0,00	0,32	3,06	0,01	0,00
Bio07_3141	secretory antigenic target	0,46	1,24	0,15	0,03	0,00	0,00	0,55
Bio07_3535	gamma-glutamyltranspeptidase	0,28	1,24	0,47	2,08	0,78	0,15	0,19
Bio07_419	Metal dependent hydrolase	0,32	0,22	0,85	0,00	0,07	1,04	0,63
contaminant		0,12	0,68	0,24	0,45	0,57	0,41	0,62
Bio07_204		0,00	0,00	0,61	0,00	0,00	1,44	0,53

contaminant		0,05	0,95	0,13	0,51	0,31	0,23	0,61
Bio07_924	Dihydrolipoamide dehydrogenase of branched-chain alpha keto acid	0,09	0,14	0,51	0,00	0,12	1,07	0,39
Bio07_333	Thioredoxin	1,16	0,22	0,26	0,03	0,31	0,00	0,00
Bio07_4267	Long chain acyl-CoA dehydrogenase	3,61	0,01	0,05	0,00	0,09	0,02	0,60
Bio07_1901	triosephosphate isomerase	1,84	0,26	0,64	0,01	0,00	0,00	0,25
Bio07_370	putative aminopeptidase YsdC	0,21	0,15	0,50	0,01	0,06	0,79	0,18
Bio07_2781		0,00	0,05	0,06	0,00	0,04	0,43	1,80
Bio07_4076	glyceraldehyde-3-phosphate ketol-isomerase	2,61	0,07	0,21	0,00	0,01	0,32	0,10
Bio07_3658	Arabinozylan arbainofuranohydrolase	0,12	0,08	0,21	0,08	0,75	0,42	0,04
Bio07_3562	Pectin lyase	0,09	0,01	0,08	0,05	1,17	0,01	0,33
Bio07_630	Purine nucleoside phosphorylase	0,22	0,07	0,37	0,00	0,12	0,69	0,15
Bio07_2599		0,02	0,14	0,54	0,00	0,02	0,32	0,60
Bio07_3316	uncharacterized protein	0,02	0,23	0,10	0,58	0,68	0,13	0,22
Bio07_653	3-phytase	0,43	0,31	0,02	0,18	0,81	0,00	0,00
contaminant		0,02	0,31	0,18	0,09	0,27	0,15	0,43
Bio07_2142	6-phosphogluconolactonase	0,44	0,16	0,45	0,00	0,00	0,26	0,06
Bio07_1717	hypothetical protein	0,66	0,25	0,07	0,04	0,54	0,00	0,01
contaminant		0,07	0,40	0,10	0,18	0,24	0,26	0,29
Bio07_369	Arabinan endo-1,5-alpha-L-arabinosidase	0,03	0,52	0,18	0,05	0,30	0,16	0,16
Bio07_916	Arginine-binding extracellular protein	0,29	0,41	0,17	0,26	0,48	0,00	0,02
contaminant		0,00	0,00	0,00	0,00	0,00	0,00	2,47
Bio07_3269	Uncharacterized oxidoreductase	0,27	0,11	0,67	0,00	0,04	0,00	0,09
Bio07_3138	uncharacterized protein	0,05	0,46	0,43	0,02	0,14	0,00	0,01
Bio07_2014	Alkyl hydroperoxide reductase subunit C-like protein	0,04	0,20	0,45	0,00	0,14	0,21	0,02
Bio07_1708	Glutamine synthetase type I	3,12	0,00	0,00	0,00	0,00	0,01	0,07
Bio07_2723	Arginyl aminopeptidase	0,00	0,03	0,10	3,29	0,16	0,20	0,05
Bio07_2792		0,00	0,00	0,42	0,00	0,07	0,55	0,06
Bio07_1884		0,00	0,03	0,04	0,03	0,84	0,05	0,06
contaminant		0,02	0,34	0,08	0,68	0,05	0,07	0,44
Bio07_744		0,00	0,65	0,05	0,14	0,21	0,02	0,00
Bio07_1321	Glutamyl endopeptidase precursor	0,00	0,10	0,25	1,37	0,05	0,26	0,08
Bio07_2151		0,00	0,17	0,22	0,00	0,00	0,21	0,46
contaminant		0,00	0,00	0,00	0,00	0,00	0,01	1,84
Bio07_698	Thermostable carboxypeptidasse 1	0,21	0,11	0,33	0,00	0,08	0,21	0,11
Bio07_1939	FMN-dependent NADH-azoreductase	0,08	0,00	0,12	0,00	0,01	0,00	1,25
Bio07_1684	serine protease APRX	0,00	0,01	0,47	0,00	0,08	0,29	0,08
Bio07_153	membrane protein related metalloprotease	0,01	0,02	0,01	0,31	0,72	0,00	0,00
Bio07_908	uncharacterized protease	0,46	0,16	0,23	0,01	0,04	0,12	0,05
Bio07_1257	Tellurium resistance protein	1,06	0,03	0,00	0,03	0,05	0,00	0,02
Bio07_703	4-deoxy-L-threo-5-hexosulose-uronate ketol-isomerase	0,05	0,13	0,23	0,00	0,00	0,40	0,06
Bio07_1338	Class D beta-lactamase	0,03	0,17	0,11	0,05	0,11	0,19	0,35
Bio07_152	membrane protein related metalloprotease	0,01	0,04	0,05	0,03	0,65	0,01	0,00
Bio07_3127	Cytosol aminopeptidase	0,29	0,23	0,15	0,00	0,06	0,02	0,24
Bio07_1655	Uncharacterized zinc protease	0,41	0,10	0,21	0,00	0,00	0,05	0,02
Bio07_548	DNA protection during starvation	0,15	0,11	0,18	0,00	0,00	0,37	0,09
Bio07_2795	delta-1-pyrroline-5-carboxylate dehydrogenase	0,00	0,13	0,32	0,00	0,12	0,02	0,08
Bio07_3842	Arginase	0,10	0,09	0,19	0,00	0,03	0,24	0,06
Bio07_4070	5-deoxy-glucuronate isomerase	1,85	0,02	0,03	0,00	0,02	0,00	0,00
Bio07_4239	methionine ABC transporter	0,27	0,00	0,00	0,00	0,22	0,04	0,69
Bio07_3560	Expasin	0,70	0,04	0,03	0,00	0,25	0,00	0,19
Bio07_1258	Tellurium resistance protein	0,43	0,14	0,11	0,01	0,04	0,00	0,29

contaminant		0,01	0,02	0,05	0,90	0,13	0,04	0,38
Bio07_1417	Peptide deformylase	0,04	0,05	0,29	0,01	0,06	0,13	0,13
Bio07_926	branched-chain amino acid dehydrogenase	0,52	0,08	0,11	0,00	0,00	0,06	0,32
Bio07_1970	Oxalate decarbixylase	0,00	0,01	0,19	0,00	0,08	0,39	0,02
contaminant		0,10	0,00	0,03	0,96	0,14	0,00	0,03
Bio07_3389	Fructose bisphosphate aldolase class	1,75	0,03	0,00	0,00	0,00	0,00	0,00
Bio07_1786	Flagellin protein FlaA	0,38	0,06	0,05	0,08	0,31	0,02	0,00
Bio07_3579	uncharacterized protein	0,01	0,09	0,08	0,11	0,36	0,02	0,00

Table 23- summary of the proteins detected in the supernatant of the bioreactor growth test, >0,1% of intensity in at least one of the sample; the test classification C1-C7 correspond to the growth parameters reported on Table 2.

REFERENCES

Aldema-Ramos, M. L., & Liu, C. K. (2010). A novel system of removing decorin, a minor proteoglycan of bovine hides, to improve the quality of leather. *Journal of the American Leather Chemists Association*, *105*(07), 222-228.

Bernfeld, P. (1955). Amylases, alpha and beta. *Methods in enzymology I*, 149-158.

Beynon J, Bod JS (1989) Proteolytic enzymes, a practical approach. IRL press, New York

Breitkreutz, D., Mirancea, N., & Nischt, R. (2009). Basement membranes in skin: unique matrix structures with diverse functions?. *Histochemistry and cell biology*, *132*(1), 1-10.

Cantera, C. S. (2001). Hair-saving unhairing process. Part 1. Epidermis and the characteristics of bovine hair. *Journal of the Society of Leather Technologists and Chemists*, *85*(1), 1-5.

Caporaso, J. G., Lauber, C. L., Walters, W. A., Berg-Lyons, D., Huntley, J., Fierer, N., ... & Knight, R. (2012). Ultra-high-throughput microbial community analysis on the Illumina HiSeq and MiSeq platforms. *The ISME journal*, *6*(8), 1621-1624.

Chavira, R. Jr., Burnett, T.J., and Hageman, J.H. (1984) *Analytical Biochemistry* **136**, 446-450

Covington, A. D. (2009). *Tanning chemistry: the science of leather*. Royal Society of Chemistry.

Dani spa, The Production Cycle, https://www.gruppodani.com/produzione/

E. N. Marieb et al., *Human Anatomy & Physiology*, 7th ed. (Pearson Internetional Edition, San Francisco, 2006) Ch.5, 152-170.

Ellman, G. L. (1959). Tissue sulfhydryl groups. *Archives of biochemistry and biophysics*, *82*(1), 70-77.

Jayanthi, D., Victor, J.S., Chellan, R. *et al.* Green processing: minimising harmful substances in leather making. *Environ Sci Pollut Res* **26,** 6782–6790 (2019).

Jianzhong M, Hou X, Dangge G, Bin L, Jing Z (2014) Greener approach to efficient leather soaking processes: role of enzymes and their synergistic effect. J clean prod 78:226–232

Jin, H. S., Park, S. Y., Kim, K., Lee, Y. J., Nam, G. W., Kang, N. J., & Lee, D. W. (2017). Development of a keratinase activity assay using recombinant chicken feather keratin substrates. *PloS one*, *12*(2), e0172712.

José Juan Almagro Armenteros, Konstantinos D. Tsirigos, Casper Kaae Sønderby, Thomas Nordahl Petersen, Ole Winther, Søren Brunak, Gunnar von Heijne and Henrik Nielsen. *Nature Biotechnology*, **37**, 420-423, doi:10.1038/s41587-019-0036-z (2019)

Kandasamy, N., Velmurugan, P., Sundarvel, A., Raghava, R. J., Bangaru, C., & Palanisamy, T. (2012). Eco-benign enzymatic dehairing of goatskins utilizing a protease from a Pseudomonas fluorescens species isolated from fish visceral waste. *Journal of Cleaner Production*, *25*, 27-33.

Khandelwal, H. B., More, S. V., Kalal, K. M., & Laxman, R. S. (2015). Eco-friendly enzymatic dehairing of skins and hides by *C. brefeldianus* protease. *Clean Technologies and Environmental Policy*, *17*(2), 393-405.

Kuntzel, A., & Stirtz, T. (1958). Hair Roots Studies. *JALCA, 53*, *445*.

Mwinyihija, M. (2010). *Ecotoxicological diagnosis in the tanning industry*. Springer Science & Business Media.
needed step towards greener technology. J Clean Prod 54:315–322

Papadopoulos, M. C. (1986). The effect of enzymatic treatment on amino acid content and nitrogen characteristics of feather meal. *Animal feed science and technology*, *16*(1-2), 151-156.

Popescu, C., & Höcker, H. (2007). Hair—the most sophisticated biological composite material. *Chemical Society Reviews*, *36*(8), 1282-1291.

Puchtler H, Waldrop FW. Silver impregnation methods for reticulum fibers and reticulin: a re-investigation of their origins and specificity. Histochemistry. 1978

Rajamani, S., & Hilda, A. (1987). Plate assay to screen fungi for proteolytic activity. *Current Science*, *56*(22), 1179-1181.

Ranjithkumar A, Durga J, Ramesh R, Rose C, Muralidharan C. Cleaner processing: a sulphide-free approach for depilation of skins. Environ Sci Pollut Res Int. 2017 Jan;24(1):180-188.

Report 2019, UNIC, https://www.unic.it/

Rodriguez-R, L. M., & Konstantinidis, K. T. (2014). Bypassing cultivation to identify bacterial species. *Microbe*, *9*(3), 111-118.).

Saran, S., Mahajan, R. V., Kaushik, R., Isar, J., & Saxena, R. K. (2013). Enzyme mediated beam house operations of leather industry: a needed step towards greener technology. *Journal of cleaner production*, *54*, 315-322.

Song, J. Y., Kim, H. A., Kim, J. S., Kim, S. Y., Jeong, H., Kang, S. G., ... & Kim, J. F. (2012). Genome sequence of the plant growth-promoting rhizobacterium Bacillus sp. strain JS.

Uitto, J., Olsen, D. R., & Fazio, M. J. (1989). Extracellular matrix of the skin: 50 years of progress. *Journal of Investigative Dermatology*, *92*(4), S61-S77.

Valeika, V., Beleška, K., Valeikienė, V., & Kolodzeiskis, V. (2009). An approach to cleaner production: from hair burning to hair saving using a lime-free unhairing system. *Journal of Cleaner Production*, *17*(2), 214-221.

Wainwright, M. (1982). A new method for determining the microbial degradation of keratin in soils. *Experientia*, *38*(2), 243-244.Cosentino S, Voldby Larsen M, Møller Aarestrup F, Lund O (2013) PLoS ONE 8(10): e77302.

Wanyonyi, W. C., & Mulaa, F. J. (2019). Alkaliphilic enzymes and their application in novel leather processing technology for next-generation tanneries. In *Alkaliphiles in Biotechnology* (pp. 195-220). Springer, Cham.

Wells, H. C., Holmes, G., & Haverkamp, R. G. (2016). Looseness in bovine leather: microstructural characterization. *Journal of the Science of Food and Agriculture*, *96*(8), 2731-2736.

Wu, Y., Guo, W., Zhao, J., Ding, L., & Chen, X. (2018). Isolation and identification of a novel LCI like antibacterial protein from Bacillus sp. MD-5 reveals its potential application in controlling Staphylococcus aureus in food industry. *Food Control*, *89*, 142-149.

Yamamura, S., Morita, Y., Hasan, Q., Yokoyama, K., & Tamiya, E. (2002). Keratin degradation: a cooperative action of two enzymes from Stenotrophomonas sp. *Biochemical and biophysical research communications*, *294*(5), 1138-1143.

Yang, C. C., & Cotsarelis, G. (2010). Review of hair follicle dermal cells. *Journal of dermatological science*, *57*(1), 2-11.

Yang, F. C., Zhang, Y., & Rheinstädter, M. C. (2014). The structure of people's hair. *PeerJ*, *2*, e619.

Yates j.R., Studies in depilation. Part X. The mechanism of the enzyme depilation process. J. Soc. Leather Technol. Chem. 56 (1972) 158-175.

ACKNOWLEDGMENTS

At the end of this long, tough, challenging but ground-breaking journey, I would like to express my gratitude to all those who have contribute to this work.

To professor Quattrone who allowed me to join this research and to professor Jousson who follow me through the difficulties of the project.

To professor Marco Gaspari for his professionality and availability to participate in the research work.

To Marco Pistocchi and the Biosphere team who greatly support me, offering their expertise and friendship.

To the CIBIO team: Mattia, Davide, Renato, Irene, Alfonso, for the precious help in the early stages of my researcher life.

To my family Lorenza, Marco, Anna and Alessio for their constant patience in supporting me. For the unconditional love, they always gave and give to me every day, even with only a glance.

To my friends in Siena Beatrice, Sara, Chiara, Silvia, Federica and Bianca, for the positive vibes that help me face the challenge.

I would like to reserve a special thanks to the Biodermol Team:

To Dario and Mauro Baruchelli, because without their vision of a sustainable future this work would not have existed.

To Paola who inspire me and help me discover more about the power of women. I found a true friend, so precious that I will keep it with me.

To Nicola who supports me during the bad days, smiling at the morning and showing me the real Veneto's lifestyle. Buy books, not cell phones.

To Mattia, Stefania, Elisa, Luciana, Rita, Tamara, Daniele, Mihail, Seydou, Elijah, for the funny time spent together. To Franco for wise advice and expert guidance in a field new to me.

You were all able to make me feel at home, Biodermol is not a workplace for me it's a crazy family.

Last but not least, to Mauro who deeply believes in this project but also in the two of us.
Only those who dare can fly.